SYNTHESIS OF DOXORUBICIN-ABLUMIN CONJUGATES VIA COBALT COORDINATION CHEMISTRY: THE EFFECT OF REACTION CONDITIONS ON OVERALL PROTEIN STABILITY

A THESIS

SUBMITTED IN PARTIAL FULFILLMENT OF THE REQUIREMENTS

FOR THE DEGREE OF MASTER OF SCIENCE

IN GRADUATE SCHOOL OF THE

TEXAS WOMAN'S UNIVERSITY

DEPARTMENT OF CHEMISTRY AND BIOCHEMISTRY

COLLEGE OF ARTS AND SCIENCE

BY

AVIONE MCGHEE B.S.

DENTON, TEXAS

AUGUST 2020

DEDICATION

I dedicate my thesis to my family and friends who supported me along the way. I would like to thank my mother for all of her kindness and knowledge. Thank you for everything you do.

ACKNOWLEDGEMENTS

I would like to, first, thank my advisor, Dr. Robby Petros. I appreciate everything you have taught me since I was an undergrad in your lab. I could not thank you more for believing in me, and seeing the greatness, in me, that I could not see in myself. I will truly miss your guidance.

I would like to thank Jason Hoshikawa for teaching me how to use the HPLC instrument. I would not have been able to do much without his expertise.

I would like to also thank Dr. Yunxiang Li for his expertise with the HPLC instrument. Thank you for being there to answer every single one of my questions. Thank you for listening and giving me great advice, and, most importantly, troubleshooting the instrument every single time I asked. I cannot thank you enough for your kindness.

I would like to thank Dr. Mary Anderson for pushing me as a student. I would have never known the caliber of my intelligence if it were not for you. Thank you for your advice and caring so much for your students. I truly appreciate it.

I would like to thank my thesis committee, Dr. Robby Petros, Dr. Nasrin Mirsaleh-Kohan, and Dr. Richard Sheardy for being there for me every step of the way. I would also like to thank them for believing in me and wanting nothing but the best for me. My time with you all will truly be cherished.

Thank you, Skylar Wappes and Sara Williams, for your support. Grad school would not have been the same without you two.

ABSTRACT

AVIONE MCGHEE

SYNTHESIS OF DOXORUBICIN– ALBUMIN CONJUGATES VIA COBALT COORDINATION CHEMISTRY: THE EFFECT OF REACTION CONDITIONS ON OVERALL PROTEIN STABILITY

AUGUST 2020

Polymer-drug conjugates have become a common tool in therapeutics to reduce the chances of pharmacotoxicity, often seen in patients undergoing chemotherapy, and to enhance targeted drug delivery. The demand for more novel forms of drug delivery has increased the efforts to develop new drug designs. Our research utilizes cobalt coordination chemistry for the synthesis of protein-drug conjugates. More specifically, this researched was aimed at crosslinking human serum albumin (HSA) and Doxorubicin via cobalt coordination chemistry. In a reversible reaction, cobalt can be used to crosslink amine-containing molecules; such as the primary amine contained in Doxorubicin and the lysine residue of HSA, via coordinate covalent bonding.

The ultimate goal of this research endeavor is to alter the biodistribution of Dox in vivo to reduce the systemic toxicity of the drug, which displays dose limiting cardiotoxicity. The use of high-performance liquid chromatography (HPLC) and dynamic light scattering (DLS) were used in identifying optimal reaction conditions for the synthesis of an HAS-Dox conjugate.

TABLE OF CONTENTS

List of tables

List of figures

CHAPTER I

INTRODUCTION

Introduction

Cancer is a worldwide disease that has been threatening human health for centuries.[1] This noncommunicable disease decreases the quality of life and the survival expectations. According to the World Health Organization, there were 9.6 million deaths in 2018.[2] Currently, the most common cancer therapies include intense practices such as chemotherapy, radiology, and surgery. Although these techniques may help, some unfortunately do not. Radiology takes a toll on the human body and weakens the patient's recovery, surgery usually does not remove all cancer cells from the body, leading to recurrence in many patients. Chemotherapeutic agents, along with radiology, typically exhibit severe toxic side effects. Chemotherapeutic drugs come with a few limitations, the highest in priority being the off-target toxicity. Some of the most common drugs like doxorubicin, cisplatin, carboplatin and docetaxel, induce severe side effects including heart damage, kidney damage, serious hemorrhaging and neutropenia, respectively. Dosage limits are typically set at the maximum amount tolerated by the patient based on systemic toxicity (i.e., the maximum amount that can be given without killing the patient). Further complicating treatment, many patients develop resistance to individual antineoplastic drugs leading to the need for multiple treatment regimes.[3] Another limitation is the low concentration of drug that can be achieved at the diseased site, and the relatively short circulation time of the therapeutics themselves. Chemotherapeutic

drugs, because of their relatively small size, can escape circulation virtually anywhere in the bloodstream upon i.v. administration leading to rapid, wide distribution throughout the body and thus short circulation times.[4] There is a pressing need in medicine for more drug alternatives and the development of more effective pharmaceuticals that induce less systemic toxicity. As a result, the current approach of utilizing nanotechnology to address some of these shortcomings has gained in popularity.

Recently, nanotechnology has been used with great success in the design of materials for use in advanced applications like material science, photonics, and drug delivery. This has led to the development of a wide body of research into the synthesis of a variety of types of nanoparticles.[1] Size can be of paramount importance for nanomaterials depending on the application; however, in general nanoparticle engineering refers to any specific engineering technique that results in uniform sized particles, ranging from 1nm to 1000 nm.[4] Nanoparticle size is a very important design parameter in the field of targeted drug delivery. To ensure extended circulation time in the body, particle size must not be too large or too small. Larger nanoparticles (>200 nm) are taken up by the reticuloendothelial system (RES), which is made up of Kupffer cells in the liver and spleen macrophages.[4,5] Smaller nanoparticles (<10 nm) run the risk of being expelled from the body via the kidneys. In addition to particle size, the propensity for accumulation of the nanoparticle into the cell is dependent on specific proteins adsorbed to the surface of the particle. Precise engineering of the surface characteristics of the particle can be used to influence the types of proteins that adsorb to it, through a

process known as opsonization, which occurs immediately after the nanoparticle makes contact with plasma.

The first synthesis of a drug delivery vector, which was a polymer-drug conjugate, can be traced back to the 1950s. During this time, polyvinylpyrrolidone was prepared as a mescaline conjugate containing a short peptide spacer between the drug and polymer that served as an enzymatically cleavable site in the construct.[5] It was seen that without the spacer, there was no release of drug from the polymer *in vivo*, but with the spacer release was observed. The conjugate exhibited sustained release in vivo resulting in higher plasma levels of the drug for a much longer duration than the similarly administered free compound. The research outlined details our efforts to synthesize and characterize a polymer-drug conjugate. To be specific, we are utilizing the protein albumin as our polymer and Doxorubicin as our drug. Furthermore, we replaced the short peptide spacer with an inorganic analogue. The albumin–Doxorubicin conjugate was synthesized using cobalt coordination chemistry, which couples an amine group on the doxorubicin with amines on human serum albumin (HSA; see Figure 1). The amine group of doxorubicin was attached to one side of our linker and albumin's amino terminus of the lysine residues was attached to the other side of the linker.[5,6]

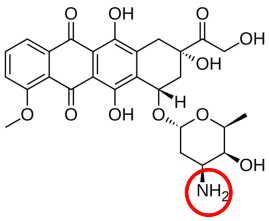

Figure 1. Chemical structure of Doxorubicin with amine group circled in red.

Doxorubicin and Chemotherapeutic Drugs

Doxorubicin (Dox), which is a 14-hydroxylated version of daunorubicin, is a red crystalline solid that was discovered in the 1950s when an Italian research laboratory isolated the anticancer compound from a microbe found in 13th century castle soil. They noticed that it exhibited positive activity against marine tumors and decided to research more into the compound. At the same time in France, researchers found the same compound, and when put together, the name became Daunorubicin as a result of "*dauni,*" a word for a famous Roman tribe and "*rubis*," which is French for the color red.[7] Doxorubicin is an anthracycline antibiotic with antineoplastic activity. It was isolated from the bacterium *Streptomyces pencetius var caesius*, and, today, it is used as an anthracycline topoisomerase II inhibitor. The enzyme alters the supercoiled DNA molecules, intercalating between the base pairs of the helix, preventing the phosphate ester linkage between the DNA strands, and, furthermore, inhibiting DNA replication and protein synthesis.[8] Doxorubicin, although useful as an anticancer drug, it is known to be cytotoxic. This is a result of the formation of oxygen free radicals. These free radicals induce cytotoxicity through lipid peroxidation (oxidative-degradation of lipids). The free radicals remove an electron from membrane lipids, resulting in membrane damage. This leads to cardiac and cutaneous vasculature effects. The reactive oxygen species (ROS) interactions with iron result in damage to myocytes causing cardiotoxicity, which is the dose limiting toxicity that is observed commonly in patients.[8]

Paclitaxel is another chemotherapy medication. The albumin-bound formation of the drug is known as Abraxane. It is a nanoparticle albumin-bound, resulting from a

water-soluble galenic formulation.[9] After it is administered, the nanoparticle rapidly disperses and activates HSA with paclitaxel molecules. Abraxane was the first albumin-based drug delivery system, which was FDA approved in 2005.[9] When approved, it was predominantly used for the treatment of metastatic breast cancer and was later used on non-small cell lung cancer. The benefit of utilizing albumin-based treatment was the overall increase in the survival of cancer patients by 1-2 months. The improved quality of life shows the progress that this form of cancer treatment can achieve.

Triggered Release and Targeted Drug Delivery

Because of the toxicity commonly associated with chemotherapeutic drugs, and Doxorubicin in particular, polymer-drug conjugates are very appealing in targeted drug delivery. Targeted delivery techniques can be used to more directly transport the drug to the tumor cell. As mentioned previously, the small size of drug molecules allows them to extravasate through tight junctions between endothelial cells lining the vasculature. Conjugation of the Dox to albumin results in a conjugate that is too large to traverse such junctions thereby restricting wide distribution and keeping the Dox confined to the circulatory system. This one feature should reduce overall systemic toxicity and improve patient response to the therapeutic. In addition, drug delivery vectors can capitalize on the EPR effect (enhanced permeability and retention effect) to selectively accumulate near tumors.[1] The enhanced permeability is a result of the "leaky" underdeveloped tumor vasculature, which permits macromolecules up to 300 nm in size to escape circulation in these newly forming vessels. Tumors also have an inefficient lymphatic system, which

drains away from the tumor leading to the selective retention of macromolecules at the tumor site.[5]

In our research, we are also capitalizing on HSA as a targeting agent. Albumin has several unique qualities that aids in its overall use for targeted drug delivery. It is known to be a natural carrier of hydrophobic molecules with favorable, noncovalent binding sites.[10] It has a very large concentration within the human body and is the most abundant serum protein.[6] The HSA, a monomeric protein with a molecular weight of 66.5 kD, is shaped like a heart with three domains and each domain having two sub-domains. HSA's primary structure consists of 585 amino acids with its overall tertiary structure comprised mostly of α-helices. The structure has 17 disulfide bridges with one free sulfhydryl on a cysteine residue.[11] These features make albumin an ideal carrier for drug loading. Moreover, the receptor for albumin, glycoprotein (GP60) receptor (albondin), is an over-expressed receptor on many different cancer cells making the HSA—Dox conjugate inherently targeting to these types of cancer cells.[6]

There are a few methods of triggered release that could have been utilized instead of the cobalt coordination chemistry employed here that uses a reductive environment for release. ATP triggered release is also a popular method, using active targeting and stimuli responsive drug delivery. The drug accumulates at the tumor site and then an external-stimulus (temperature, light, or magnetic field) facilitates the release of the drug. Gold-based nanostructures commonly utilize absorption by plasmon resonance or "light-based therapeutics," and surface enhancement by SERS (Surface-Enhanced Raman spectroscopy) to confirm drug loading. To ensure that the nanoparticle releases the drug,

infrared light is focused at the desired site to trigger release. Another strategy uses thermally sensitive liposome loaded with drugs. Localized heating then triggers the release of the drug from the liposomes and was also shown to increase drug uptake and penetration into tumor cells. Another commonly utilized delivery vector consists of antibody drug conjugates, which are known for their high degree of specificity in targeting and triggered release in tumor cells; however, high off-target toxicity levels have been observed in some cases.[12–15]

Conjugation of Prodrug and Protein

In our research, Doxorubicin, albumin, and our linker are considered the three parts of our polymer-drug conjugate. As the former states, albumin is sufficient for targeting and our crosslinking for our polymer and drug is based on synthesizing an inorganic Werner type complex. Cobaltous chloride hexahydrate or cobalt chloride hexaaqua complex ($CoCl_2 \bullet 6H_2O$) were used as our source of cobalt (Co). Cobalt has little toxicity and is an important component for many metalloenzymes. Initial efforts at utilizing Co in our bioconjugation technique relied on the use of a somewhat labile Co^{3+} complex that had been previously reported. However, all attempts to utilize this complex as a generic amine crosslinker were unsuccessful. A more general approach developed by our research groups utilizes $CoCl_2$, which undergoes facile ligand exchange that can then be oxidized to a more physiologically stable Co^{3+} using hydrogen peroxide leading to an exchange inert complex. Another advantage of this method is that it allows for the possible conjugation of up to six amine-containing molecules per prodrug complex whereas most other bioconjugation reagents are limited to only two.[6] Furthermore, the

conjugation reaction involves only a lone pair of electrons on the nitrogen atom of the amine, which will form a dative bond between Co and nitrogen (Figure 2). This reaction allows for the "crosslinking" between our protein, HSA, and our drug, Doxorubicin. When cobalt gets reduced back to Co^{2+}, the structure will release the amine into its native state.[6] This is hypothetically achieved by triggered release inside of the tumor cell due to the presence of much higher levels of reduced glutathione, which creates a reducing environment within the cell.

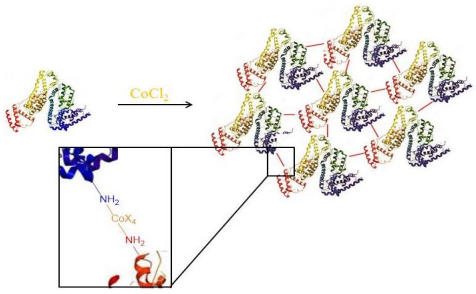

Figure 2. Structure of the synthesis process of protein nanoparticle via cobalt coordination chemistry.

Analytical Theories

Dialysis Cassette

Several techniques can be used to determine the stability of the Albumin–dox conjugate. A series of experiments were conducted to test the reagent's concentration in various solutions that allowed us to quantitatively determine the number of Dox molecules bound per protein molecule. For our research, the experiments used dialysis to determine the amount of Doxorubicin released. We used 3500 MWCO cassettes that allowed unbound Dox to freely diffuse out of the cassette. Albumin is a 65,000 MW

protein that cannot diffuse through the membrane of the cassette, and thus will be retained inside the cassette. For this procedure, we used it to remove unbound Dox and assume any Dox that was retained in the cassette must be bound to protein. Dialysis cassettes are commonly used as in buffer exchange or to remove low molecular weight contaminants. Using the cassette helps to maximize the surface area to sample volume ratio and to obtain complete sample recovery for further characterization and testing. This technique was performed using a bulk phase containing phosphate-buffered saline (PBS). A typical albumin-Dox conjugate synthesis involved mixing the following reagents: HSA, $CoCl_2 \bullet 6H_2O$, NaOH and Doxorubicin HCl.

A typical synthetic procedure is outlined in Figure 3. Separate solutions containing HSA and Dox were raised to pH 10. This change in solution pH ensured that any amines, which are utilized for crosslinking, were in the neutral form (i.e., not protonated). Next, the two solutions were mixed followed by the addition of $CoCl_2 \bullet 6H_2O$. The solution pH was again adjusted to pH 10 as necessary. A control sample was prepared by placing Dox only in a cassette and the measuring its release to the bulk phase as described below. Experiments were conducted to examine the effects of each reagent's concentration on the synthesis of the conjugate. We also examined the effect of solution pH on the overall synthesis, the effects of the order of addition of reagents, and the omission of each reagent. Each test was conducted under the theory that HSA has 59 lysine residues and of the 59, there are about 20 that accessible for covalent attachment.[11] If this is true, we hypothesized that we could vary the number of Dox molecules bound to the protein between 1 and 20. Each dialysis cassette was suspended

in 200ml of PBS for ~48 hrs. The bulk phase was then analyzed by using HPLC instrumentation.

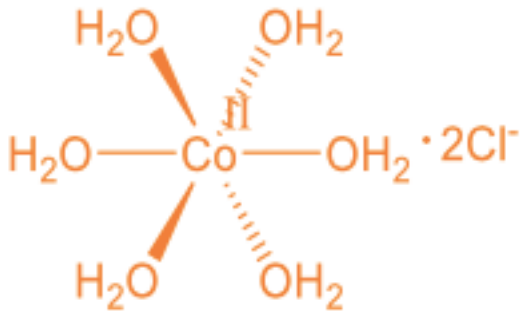

Figure 3. A model of cobalt chloride hexa-aqua complex.

HPLC Analysis

High Performance Liquid Chromatography is an analytical technique that is used to separate individual components of samples so that they can be quantified. The technique uses pressurized pumps to pass solvents through a column. The column contains a resin that is used as a separation medium via the affinity of the sample components to the particular resin in the column. More specifically, the type of HPLC that was used here was a reverse-phased technique. This is when the stationary phase (the column) is non-polar and the mobile phase (the liquid passing through) is polar. The parameters used on the instrument were very selective depending on the sample that was being tested. Doxorubicin possesses both polar and non-polar characteristics as a result of its functional groups. This means there is some attraction between the non-polar and polar phases because of the presence of both hydrophobic and hydrophilic forces. As a

result, the balance of these forces must be considered when setting the instrument's parameters. The most important criteria were the selection the mobile and stationary phases.

There was an equilibrium that must be achieved between the mobile and stationary phase, before analysis can begin. The mobile phase was set to isocratic flow, meaning the solvent mixture was constant throughout the experiment. Acetonitrile (ACN) and water were used as the mobile phase because one can easily manipulate polarity by adjusting the ratio of ACN (non-polar component) to water (polar component). A mobile phase consisting of a 70:30 mixture of water and ACN respectively was used. The stationary phase consisted of an alkyl-chained, C-18 column, which is non-polar. Before testing the bulk phases from experiments, a variety of diluted Doxorubicin and water samples were used to in order to adjust the retention time, or the amount of time the sample spent on the column, to achieve the desired separation of Dox from other components of the synthesis.

This HPLC instrument was equipped with a UV-Vis detector. The column of the HPLC serves to separate the components of the sample while UV-Vis was used to detect each component and to quantify concentration. We employed the UV/Visible detector for a few reasons. For one, we were trying to separate our sample to give us a pure compound–free doxorubicin. Doxorubicin exhibits spectral bands at 480 nm and 296 nm. We must separate the Dox from any cobalt complexes in solution because the cobalt also exhibits an absorption band in the visible region. Cobalt complexes are typically

octahedral in shape and can exchange ligands through an associative substitution reaction that is analogous to an S_N2 reaction commonly observed in organic chemistry.[16]

Because doxorubicin and the cobalt complexes have an absorbance at ~480 nm, it would difficult to quantify each in the presence of the another when using UV-Vis without first separating the two. HPLC was well suited for such a separation because the cobalt complexes were much more polar in nature and therefore easy to separate using this technique.

The instrument was used to quantify the exact amount of unbound doxorubicin molecules in the bulk phase. The unknown concentrations of Dox contained in our samples were determined by first generating a calibration curve. This was achieved by running samples of known Dox concentrations and then plotting peak area vs concentration. A linear fitting of the data generated an equation where the area observed for the unknown can be used to determine Dox concentration. Once the concentrations were determined, we calculated the amount of bound Dox from the known amount of Dox that was released compared to the total amount added to each sample. From there, one can calculate the number of Dox molecules per protein.

Dynamic Light Scattering

Dynamic light scattering (DLS) is an analytical technique that can be used to observe aggregation of protein samples by determining the size distribution of particles in solution as small as 1nm. The instrument focuses a laser beam on the sample that scatters light, which is detected at an angle by a photon detector.[18] We employed DLS in our research to investigate protein aggregation. Our goal was the synthesis of albumin-Dox

conjugates that are themselves stable in solution. Protein aggregation needed to be avoided as it hampers the development of biopharmaceuticals. Proteins have a natural propensity to aggregate depending on changes to solutions, and with DLS we could investigate whether this problem had occurred and potentially develop methods to reverse it or avoid it altogether.

Dynamic light scattering is used both in physics and chemistry to determine size distribution. The theory when light impinges on a molecule, is that the electric field of the light creates an oscillating polarization on the electrons.[21] When utilizing the light scattering technique, this means operating a few physical principles: Brownian motion, Doppler effect, and Heterodyne detection.

Brownian motion is the random collision and motion taken on by particles suspended in a fluid. The velocity and motion of the particles are random, but the velocity distribution, a function of particle size, can be averaged over a period of time.[21] The light used in the instrument was from a laser diode, which was coupled to the sample through an optical power splitter/probe. The light was then scattered and reflected off of the particles, sent through a sapphire/fluid interface, and then transmitted to the photo-detector.[21] The scattering of light is known as Doppler-shifted light. The photomultiplier or the main source of detection, for the Doppler-shifted light, is known as Heterodyne detection. It involves combining Doppler-shifted light with a reference beam of light (the reference is not Doppler-shifted). The two sources of light are then sent through the detector and analyzed.

CHAPTER II

MATERIALS AND METHODS

High Performance Liquid Chromatography

Liquid chromatography experiments were carried out on Shimadzu CBM-20A (Shimadzu Manufacturing INC.). The instrument used was comprised of three parts: an interface or communication bus module (CBM-20), the UV/Vis detector (SPD-20AV), and the liquid chromatograph (LC-20AT) or pump. HPLC was used to determine calibration curve via integration of the area under the peak. The retrieved data was then calculated to find the molecules of Dox per HSA molecule.

Samples were inserted into the injector using a 25 µL Microliter #702 syringe (Hamilton Co., Reno, Nevada). A C-18 column (Shimadzu) was used to increase separation. The pressure for each run was set to ~1400 max psi on a low-pressure gradient. The pump flow rate was 1.00 mL/min and run times varied 5-6 minutes for each sample. The mobile phase consisted of a 70:30 ratio of ultra-pure water and acetonitrile (*Baker Analyzed*® HPLC ultra-gradient solvent). The solvent was acidified by adding phosphoric acid to the ultra-pure water in 2 µL increments until a pH of 3 was achieved. Using a 3510 Branson Sonicator, the solvent was degassed for approximately 15 minutes before it was added to the acetonitrile. An isocratic elution was the preferred mode of separation. This method was chosen after observing the formation of bubbles in the mixing chamber while performing gradient elution.

Lines were purged as needed to ensure the pump was free of bubbles and excess sample. Before each sample run, ~50 µl of ultra-pure water was injected to rinse the sample injector. For every run, ~25 µL of sample was inserted into the injection valve. Precisely, in this order, the injection valve lever was rotated before the run was activated using the software. Each sample ran for 5-6 minutes. The peaks were then integrated using the *Shimadzu LC Solutions* software. The peak areas were recorded and used for further data analysis.

Dynamic Light Scattering

Microtrac Nanotrac Wave II Particle size and ZetaPotential Analyzer (Mictrotrac Inc.) was used to test albumin size distribution and the overall stability of our polymer-drug conjugates. The *Nanotrac Wave II* instrument uses optical techniques to determine particle size, collect ZetaPotential and molecular weight[21]. The *Nanotrac Wave II* filters, digitizes and analyzes data utilizing the Microtrac FLEX windows software.

The samples analyzed via HPLC were the same sample solutions analyzed by DLS. Samples from experiments varying the pH (7-10), and cobalt concentration, and Dox concentration were analyzed. Before running DLS on the samples, a miniature vortex was used to homogenize the solution. A 3 mL Pasteur pipette was used to insert ~0.5 mL of ultra-pure water into the sample cell. To ensure that the surface was clean, this was performed before each sample was run. Once the ultra-pure water was removed, ~0.5 mL of sample was transferred to the sample cell. The temperature parameters were set to ~18.1-19.8°C. The samples were run on the autozero function to allow the sample to run as soon as the software was activated. Sample run times were 6 replicates of 30 sec

each. The results for the 6 runs were then averaged and analyzed for size distribution and Polydispersion Index (PDI) via the FLEX software.

Synthesis of Albumin-cobalt Crosslinked Nanoparticles

All albumin-cobalt crosslinked nanoparticles were synthesized by reproducing protocol from Doug T Nguyen's *Werner Complex Viewed Anew.*[6] The goal for reproducing the cobalt crosslinking project was to familiarize with the cobalt crosslinking method and reproduce previous results before moving on to new method development for a protein-drug conjugate.

Stock solutions of 0.1 M $CoCl_2 \bullet 6H_2O$ (Fischer Scientific Lot# 142533), 0.25 M NaOH, and 10 mg/mL albumin were prepared and used in all experiments. In a typical experiment, 1 mL of albumin was added to a 4 mL glass vial followed by ~50–200 µL of cobalt solution and then 20–200 uL of NaOH. Samples with varying concentrations of each reactant were then analyzed via DLS.

Through further investigation, additional methods were added to ensure exact nanoparticle size. Sonication was performed before the addition of the 0.25M NaOH solution. About 8 µL of 30% H_2O_2 was added to increase oxidation of cobalt. This method was then refined to include H_2O_2 at 0.2 µL, which resulted in a more precise size for particles.

Results proved that most efficient method for albumin-cobalt crosslinked nanoparticles was to add 1 mL of a 10 mg/mL solution of albumin and water to a 52.5 µL $CoCl_2 \bullet 6H_2O$ and 10 mg/µL of NaOH solution. This final method gave consistent particle

sizes. The parameters were then used as a starting point for further experimentation on the albumin-Dox conjugate.

Synthesis of Albumin–doxorubicin conjugates

The formation of Albumin–doxorubicin conjugates consisted of: Bovine Serum Albumin (BSA) or HSA (MP Biomedicals, LLC Lot# Q2097), Doxorubicin HCl, and $CoCl_2 \bullet 6H_2O$. Conjugates were prepared using 1 mL of the 10 mg/mL of BSA or HSA, 52.5 µL of the 0.1 M $CoCl_2 \bullet 6H_2O$, 200 µL of the Dox stock solution (5 mg/mL, Sigma Aldrich Lot# LRAB3692) and varying amounts of 70% H_2O_2 and 0.25M NaOH and HCl. For the initial set of experiments BSA was implemented as the biopolymer during conjugation, which served as a more cost-effective surrogate to the clinically relevant, and much more expensive HSA. Should this technology advance to clinical trials, HSA will be used exclusively.

After running each reaction, each sample was injected into a dialysis cassette (3,500 MWCO, 0.2–3 mL sample capacity, Slide-A-Lyzer® Lot# LE144493) using a 5 mL disposable syringe (Excelint® Lot# 141004). The dialysis cassettes were submerged in 180:20 ratio of ultrapure water and 10X solution of phosphate buffer saline (Fischer Bioreagents Lot# 153384). The samples were incubated in dialysis cassettes for 48–72 hrs at room temperature with no stirring. After further investigation displayed the significance of the amount of time in the sample buffer, parameters were adjusted. Samples were incubated for ~72 hrs to allow the complete release of unbound Dox into the bulk phase.

Our first experiments with albumin-Dox conjugation was to investigate the role of our novel crosslinker, Co. This was accomplished by preparing identical samples either with or without cobalt. Experiments that followed, examined the role of cobalt concentration in conjugation efficiency and the significance of the order of addition of reagents during synthesis.

Additional experiments examined the effects of Dox concentration and reaction pH during conjugation. Several samples at varying Dox concentrations were prepared by simply adding different amounts of the 5 mg/mL Dox stock solution to each sample. All samples were then incubated in dialysis cassettes in PBS for ~72 hrs and unbound Dox quantified via HPLC. Analysis of the effects of reaction pH on conjugation efficiency was performed by adjusting the solution pH to the desired value (by adding appropriate amounts of 0.25M NaOH and/or 0.25M HCl to manipulate pH) before the addition of cobalt, the crosslinking reagent.

Experimental results showed that the most efficient order of addition of reagents were the addition of HSA first, then Dox, followed by NaOH to raise the pH to 10. $CoCl_2 \bullet 6H_2O$ was then added followed by the addition of NaOH to raise the pH to 10. Reactions were then left undisturbed for 10 minutes before adding 70% H_2O_2 for oxidation of cobalt to its inert oxidation state, which completes the bioconjugation reaction.

Preparation of Standards

Standard solutions were used as a measurement calibration tool for each sample. The standards were prepared using either bulk phase or stock solution Dox reagents and

diluting the reagents ultra-pure water. Bulk phase standards consisted of injecting a known amount of Dox (similar amounts that were used in bioconjugation reactions) into a dialysis cassette and then collecting the bulk phase after 72 h for analysis via HPLC. Standards of varying concentrations for generating a calibration curve were prepared by diluting the bulk phase standard with various amounts of ultra-pure water. Standards prepared from bulk phase were measured and labeled as either 1:0, 1:2, 1:3, 1:5, 1:6, or 1:10 dilutions. Solution standards were also prepared by simply diluting the 5 mg/mL Dox stock solution. Using ultra-pure water, the Dox stock solution was diluted to produce 10 µg/mL, 5 µg/mL, and 1 µg/mL standards.

CHAPTER III

RESULTS AND DISCUSSIONS

HPLC Studies

Generating a Calibration Curve for Dox

A calibration curve was generated to allow us to determine the concentration of Dox in unknown samples. Briefly, samples of known concentration were run on the HPLC and peak areas recorded for each sample (runs were conducted in triplicate; see Figures 6–8). Those peak values were then plotted versus Dox concentration and fit with a linear regression analysis. This linear data fit then provided an equation that allowed us to quantitatively evaluate our data on unknown samples. The data for the calibration curve experiment was collected over a 24-hour time period (see Figures 4, 5). The purpose for this set of experiments was to test the accuracy of ability to determine the Dox concentration in each sample. Three standard solutions (10, 5, 1 μg/mL) were tested initially because this range represented the approximate range in concentrations expected for unknown samples. The area under the curve for each sample was then integrated and the values were averaged.

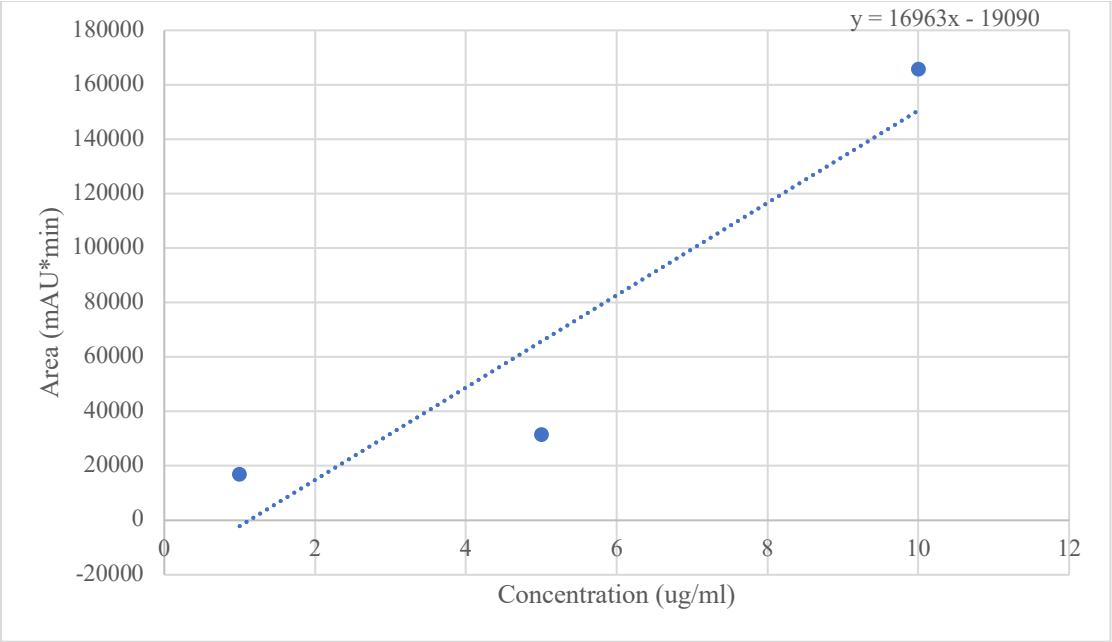

Figure 4. Concentration vs. peak area for freshly prepared Dox stock solutions at 10, 5, and 1 µg/mL.

The slope intercept equation ($y = mx+b$) was used to find the value of, x, the concentration in unknown samples. The slope intercept equation was rearranged to solve for concentration (see Equation 1). For unknown samples, the average area for each sample could be plugged in for y and the intercept for c, which was all divided by the slope, m.

$$\textit{Equation 1: } \left(x = \frac{y-c}{m}\right)$$

After 24 hours the same procedure was repeated. The peak areas were collected and averaged. A *t*-test was then used to test the data's accuracy. The two sets of data analyzed were the 10 µg/mL for Day 1 and the 10 µg/mL for Day 2. The confidence interval for the two data sets was 90%. The confidence interval shows a high degree of certainty that the data collected would fall within these values if it were tested again.

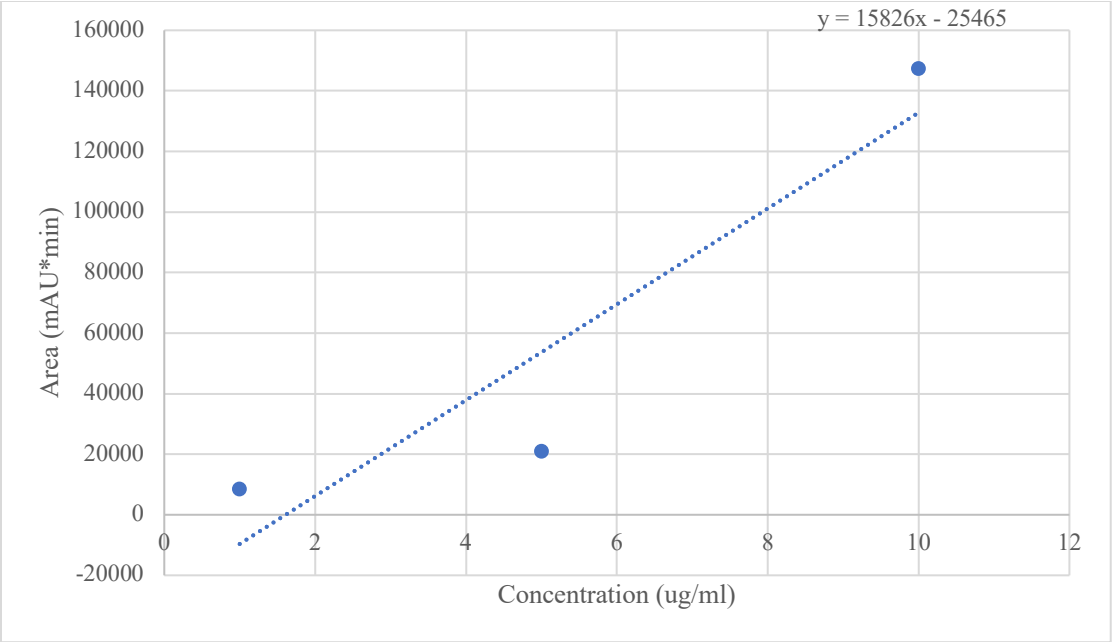

Figure 5. Concentration vs. peak area for Dox stock solutions at 10, 5, and 1 µg/mL after 24 h.

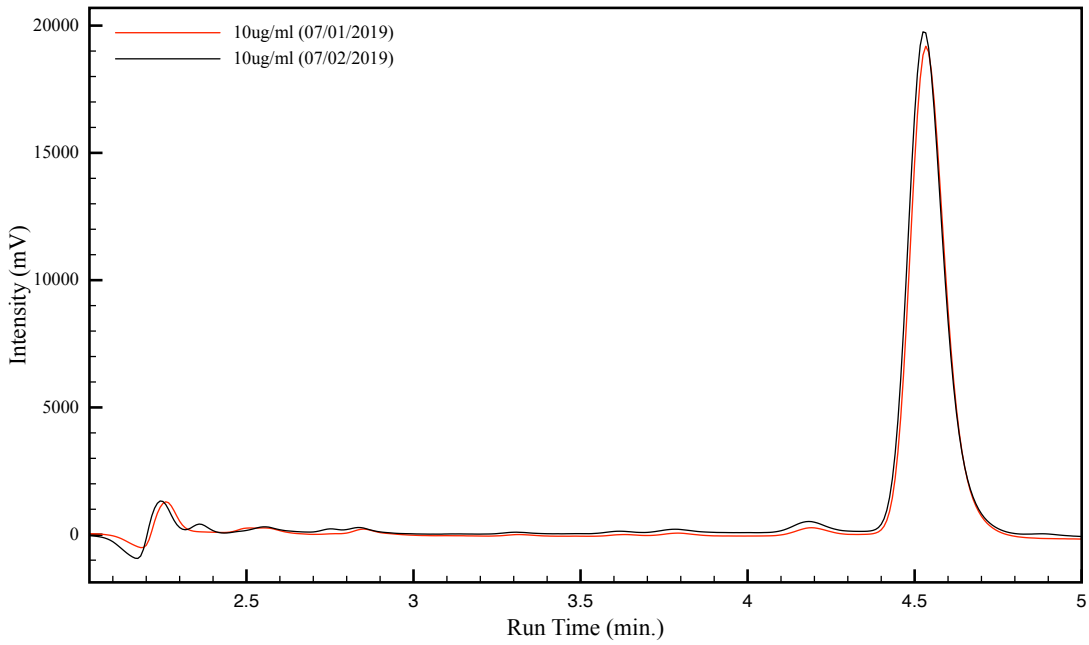

Figure 6. Chromatograms for 10 µg/mL Dox samples run immediately after preparation and the same sample after 24 h.

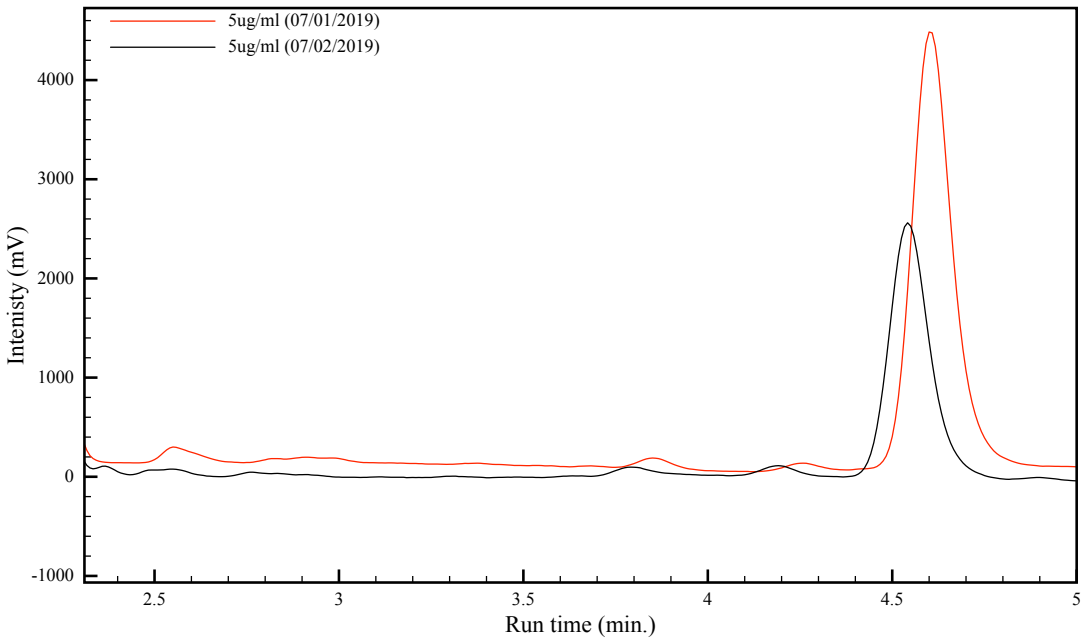

Figure 7. Chromatograms for 5 µg/mL Dox samples run immediately after preparation and the same sample after 24 h.

Data from the 5 µg/ml standards were less consistent than similar data from the 10 µg/mL samples. The average integrated areas were 31404.6 mAU*min at 4.6 min on Day 1, and 21010.07 mAU*min at 4.5min on Day 2 (see Figure 7). The sample was checked for homogeneity and was left no longer than 24 hours after preparation. Degradation could have occurred, but the concentration results differed by only 0.04 µg/ml and the average areas by only 10,000 mAU*min (see Table 1.1, 1.2). This meant the data was of sufficient quality to report, but it differed enough to warrant further study. Based on these results, we decided all data analysis would need to be done on the day of preparation.

Further evidence of this issue can be seen in Figure 8 with the 1 µg/mL standard solution. The peak area for day 2 (8503.6 mAU*min) was nearly half the area of day 1

(16940.6 mAU*min). The difference in the data, over 24 hours, was significant enough to support changes to our protocols previously mentioned.

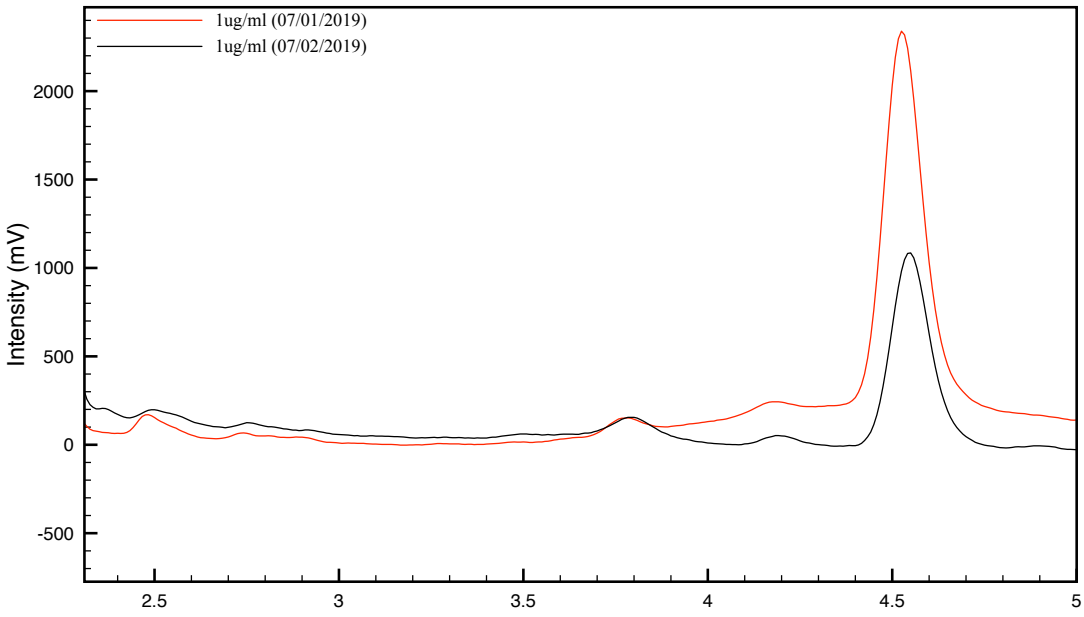

Figure 8. Chromatograms for 1 µg/mL Dox samples run immediately after preparation and the same sample after 24 h.

Table 1.1. HPLC results from Dox calibration standards on Day 1

Dilutions (µg/mL)	*Standard Concentration (µg/mL)*	*Average Area*	*Concentration from slope intercept (µg/mL)*
10	10	165796.52	10.8993
5	5	31404.6	2.97674
1	1	16940.56	2.12406

Table 1.2. HPLC results from Dox calibration standards after 24hrs

Dilutions (µg/mL)	*Standard Concentration (µg/mL)*	*Average Area*	*Concentration from slope intercept (µg/mL)*
10	10	147312.17	10.9173
5	5	21010.07	2.93662
1	1	8503.63	2.14638

Synthesis of an HSA-Dox conjugate

Three samples were prepared and were incubated in dialysis cassettes for ~72 hours. Sample #1 contained albumin and Dox, but cobalt was omitted. Sample #2 included all reagents, and Sample #3 contained only Dox. Immediately following the preparation of each standard solution, a calibration curve was generated using integrated peak area data (see Figures 9-10, Table 1.3). The resulting linear fit was then used to compute the exact concentration of Dox in the bulk phase for each sample and thereby the amount of Dox retained in each cassette (see Figure 11, Table 1.4).

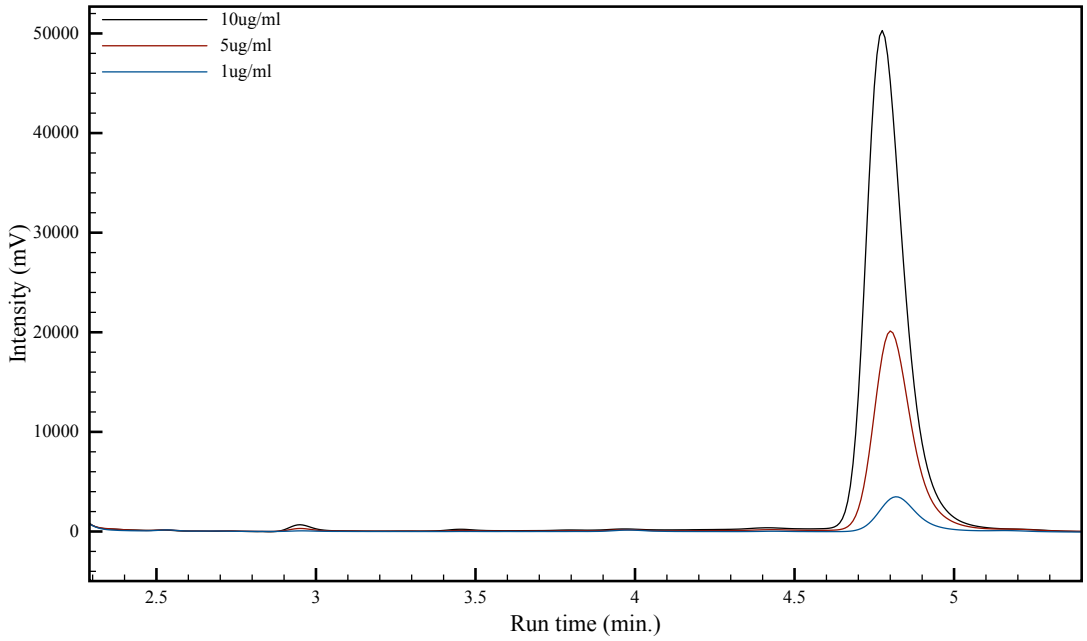

Figure 9. Chromatograms for 1, 5, and 10 µg/mL Dox samples run immediately after preparation.

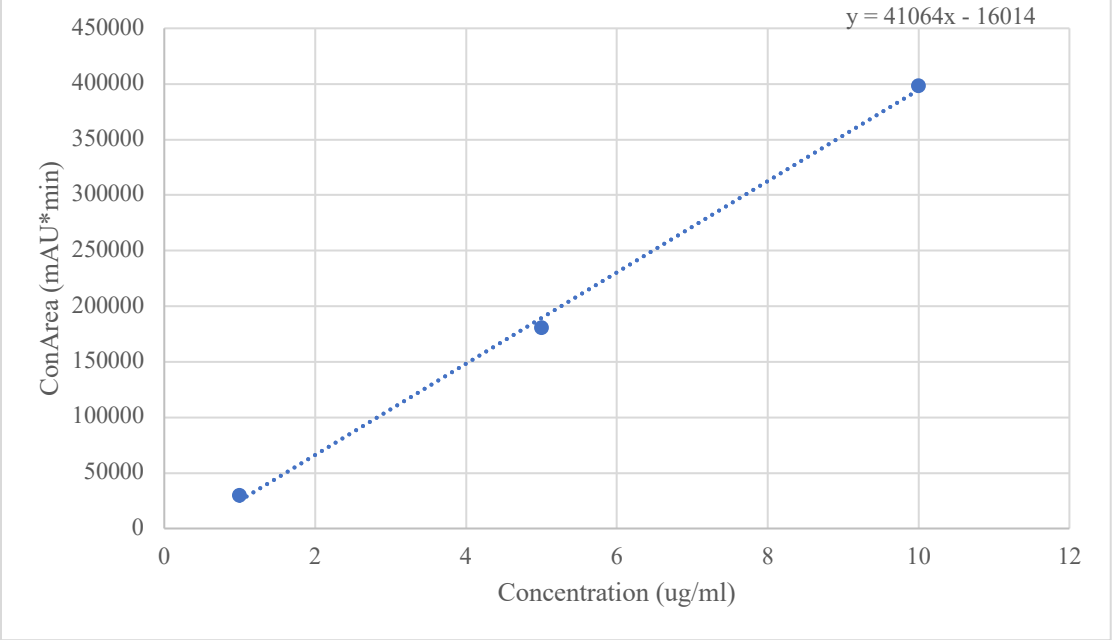

Figure 10. Concentration vs. peak area for freshly prepared Dox stock solutions at 10, 5, and 1 µg/mL.

Table 1.3. HPLC results from Dox calibration standards.

Dilutions (µg/mL)	*Standard Concentration (µg/mL)*	*Average Area*	*Concentration from slope intercept (µg/mL)*
10	10	398392.53	10.0917
5	5	180833.23	4.79367
1	1	29757.8	1.11464

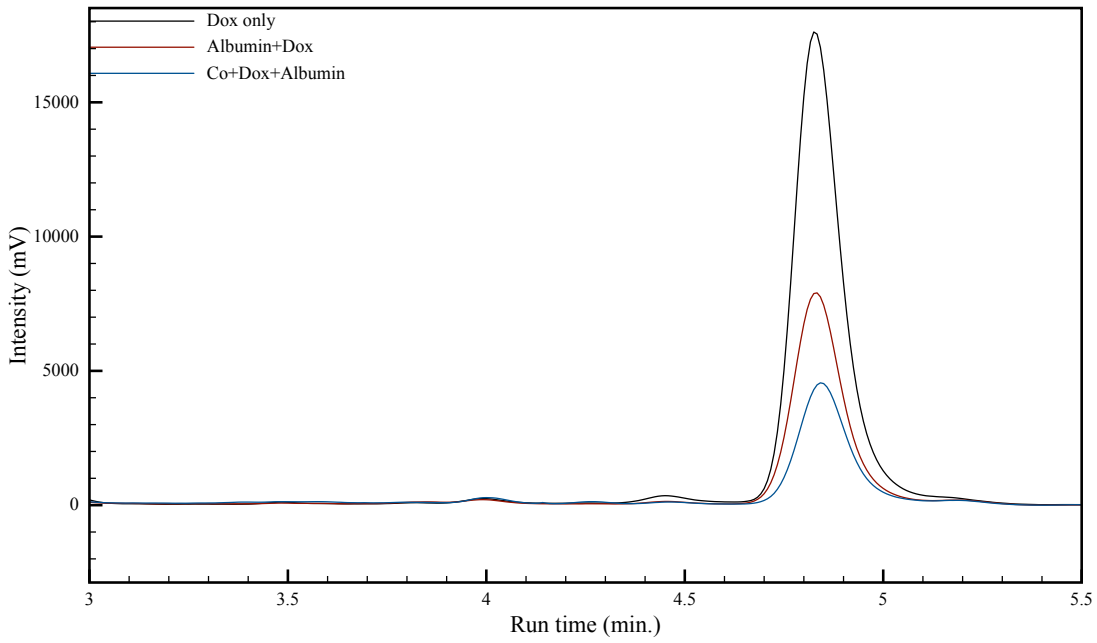

Figure 11. Chromatograms for various samples prepared for the synthesis of an HSA-Dox conjugate.

Table 1.4. HPLC results from HSA-Dox conjugate synthesis.

Sample	*Average Area*	*Concentration Dox area (µg/mL)*	*Dox released (µg)*	*Dox retained (µg)*	*mol Dox*	*%Dox retained*
Dox only	139365.5	3.784	764.3	185.7	$3.40*10^{-7}$	19.40
Alb.+Dox	82704.2	2.404	485.6	464.4	$8.54*10^{-7}$	48.88
Co+Dox+ Alb.	42252.5	0.494	99.70	850.3	$1.56*10^{-6}$	80.50

Samples 1-3 resulted in 49%, 81%, and 20% Dox retained, respectively. The "Dox-only" sample (Sample #3) or the control sample, retained the least amount of Dox as expected. This result in and of itself was problematic because theoretically all the Dox should have been released. The "*albumin+Dox*" sample (Sample #1) resulted in 5 molecules of Dox/HSA retained. Again, this is problematic because albumin is known to

have predominately 2 molecular binding sites. This result suggests that some aspect of the synthesis leads to non-specific binding of Dox to the protein in the absence of the crosslinker (Co), which is a complicating factor. In comparison, the "*cobalt+albumin+Dox*" sample (Sample #2) had double the number of Dox/HSA molecules bound. With the addition of cobalt, there is a higher probability of polymer-prodrug conjugation.

Effects of Reagents During Conjugation: Timing of Cobalt Addition

The impact of the timing of addition of cobalt to the reaction was investigated to observe the effects on overall conjugation efficiency. This was to determine if there were any significant changes in efficiency based on whether cobalt was added before or after addition of HSA. Beginning with this set of experiments, a new method was utilized for preparing Dox standards for generating calibration curves. In previous experiments, a 5 mg/mL Dox stock solution was simply diluted to the desired concentration with PBS. This method consistently underestimated the amount of Dox in bulk solutions in comparison with samples containing free Dox dialyzed for 72 hr. Given this discrepancy, we began utilizing dialyzed Dox as calibration standards. A solution containing a known amount of Dox (typically 950 mg) was added to the dialysis cassette. The sample was then dialyzed for 72 hr followed by analysis via HPLC (see Figures 12-13, Table 1.5). The assumption was made that Dox would diffuse out of the cassette until it reached the same concentration both outside and inside the cassette. This was confirmed by testing samples of the bulk phase vs. samples inside the cassette after dialysis.

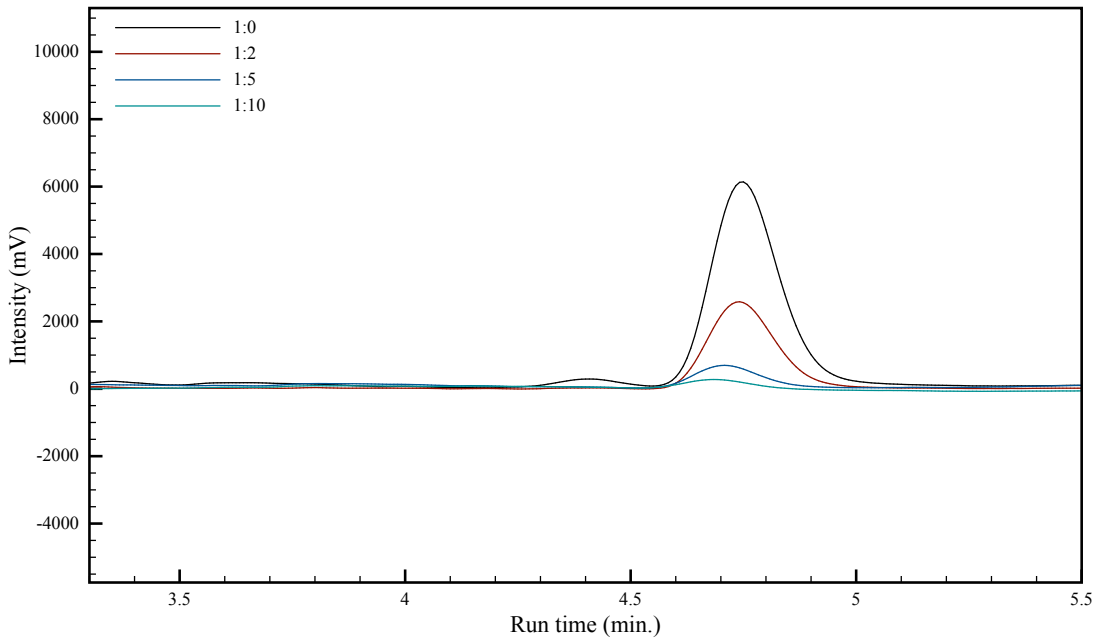

Figure 12. Chromatograms for calibration standards at various dilutions shown. Samples were collected from the bulk solution after dialysis of sample containing 950 mg Dox only. Dilutions noted were prepared using bulk phase diluted with 1x PBS.

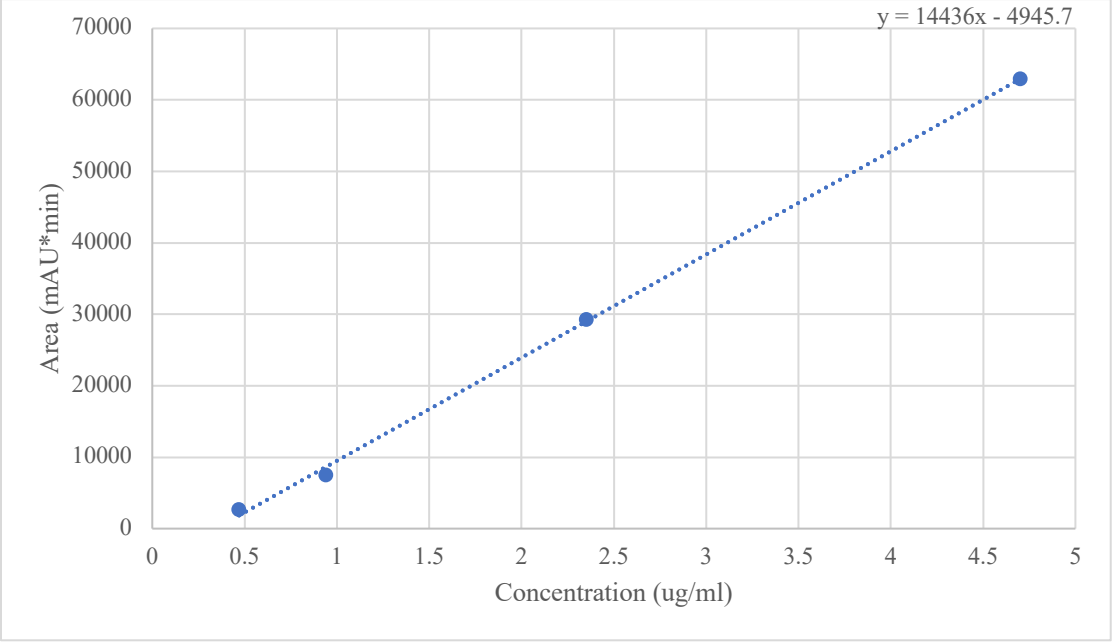

Figure 13. Calibration curve results for the timing of cobalt experiment.

Table 1.5. Data for the standard concentrations

Dilutions	*Standard Concentration (µg/mL)*	*Average Area*	*Concentration from slope intercept (µg/mL)*
1:0	4.7	62904.33	4.70005
1:2	2.35	29264.43	2.36977
1:5	0.94	7485.53	0.86112
1:10	0.47	2693.2	0.52915

In early experiments toward the synthesis of the HSA-Dox conjugate, it was found that combining Dox and HSA before raising the pH with NaOH led to significant non-specific binding of Dox to the protein. Dox was soluble at pH 5-6 and at pH 9-10; however, it was insoluble at pH 7-8. We theorized that this change in solubility led to some type of non-specific agglomeration if Dox was in the presence of protein during the pH adjustment. To minimize this possibility, solutions of Dox and HSA were adjusted to pH 10 separately and then mixed subsequently. What was not known was whether the timing of addition of cobalt would impact the reaction efficiency.

To this end, we investigated the three possibilities. First, adding cobalt to the Dox solution before adding the HSA solution. Second, adding cobalt to the HSA solution before adding the Dox solution. Or third, mixing the Dox and HSA solutions and then adding cobalt. Figure 14 shows the results for each sample. The peaks were slightly wider and less resolved than those observed in previous experiments. All peaks were observed at ~4.7 min with an intensity of ~1000 mV, meaning there is very little difference in efficiency based on order of addition.

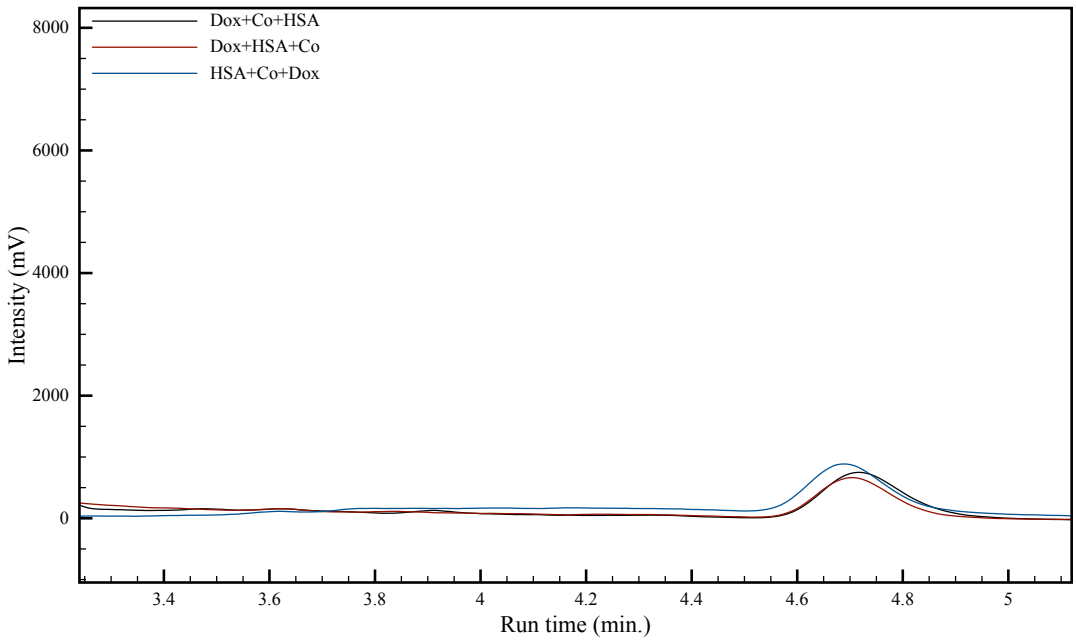

Figure 14. Chromatograms for samples examining the influence of timing of cobalt addition on conjugation efficiency.

There was roughly an 8% gain in efficiency (see Table 1.6) if the cobalt was added after mixing the other two reagents first, which was then used as the preferred method in all future experiments. It was unclear what underlying chemical reactivities led to this small difference in efficiency.

Table 1.6. Results for the Effects on the conjugation after Addition of the Cobalt Reagent

Sample	*Average Area*	*Concentration Dox area (µg/mL)*	*Dox released (µg)*	*Dox bound (µg)*	*mol Dox*	*mol Dox/HSA*	*%Dox bound*
Dox+Co+HSA	7857.85	0.887	179.15	770.8	$1.41*10^{-6}$	9.45	81.1
Dox+HSA+Co	6503.1	0.793	106.21	843.8	$1.55*10^{-6}$	10.35	88.8
HSA+Co+Dox	8242.5	0.914	184.53	765.5	$1.41*10^{-6}$	9.59	80.6

Generating a Calibration Curve for Multiple Experiments

A single calibration curve (see Figures 15-16, Table 1.7) was used to analyze the results in the next three experiments.

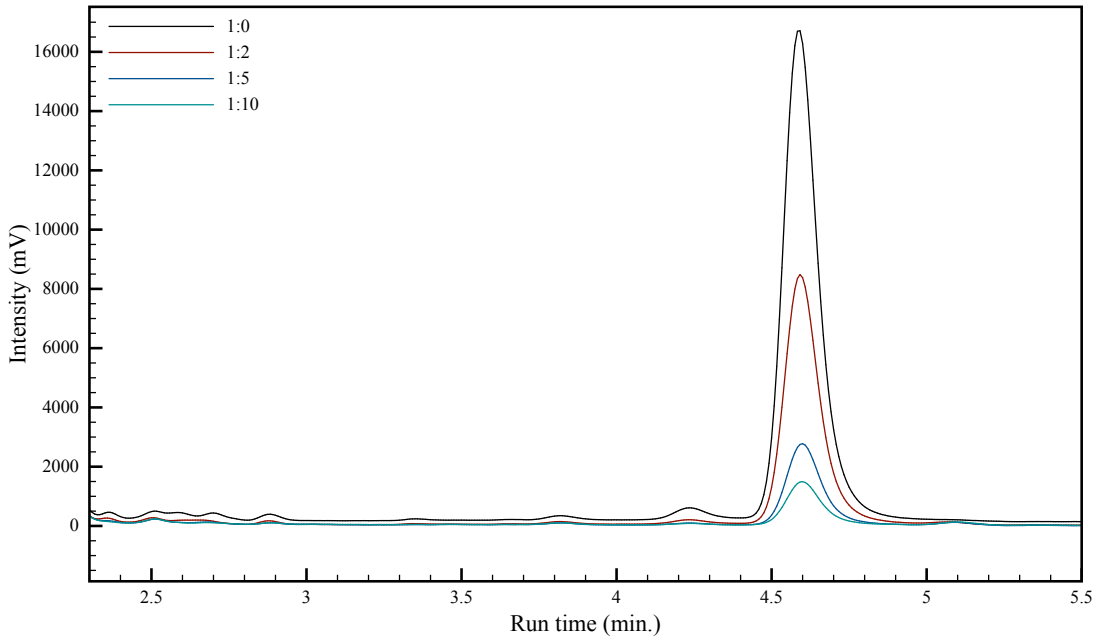

Figure 15. Chromatograms for calibration standards at various dilutions shown. Samples were collected from the bulk solution after dialysis of sample containing 950 mg Dox only. Dilutions noted were prepared using bulk phase diluted with 1x PBS.

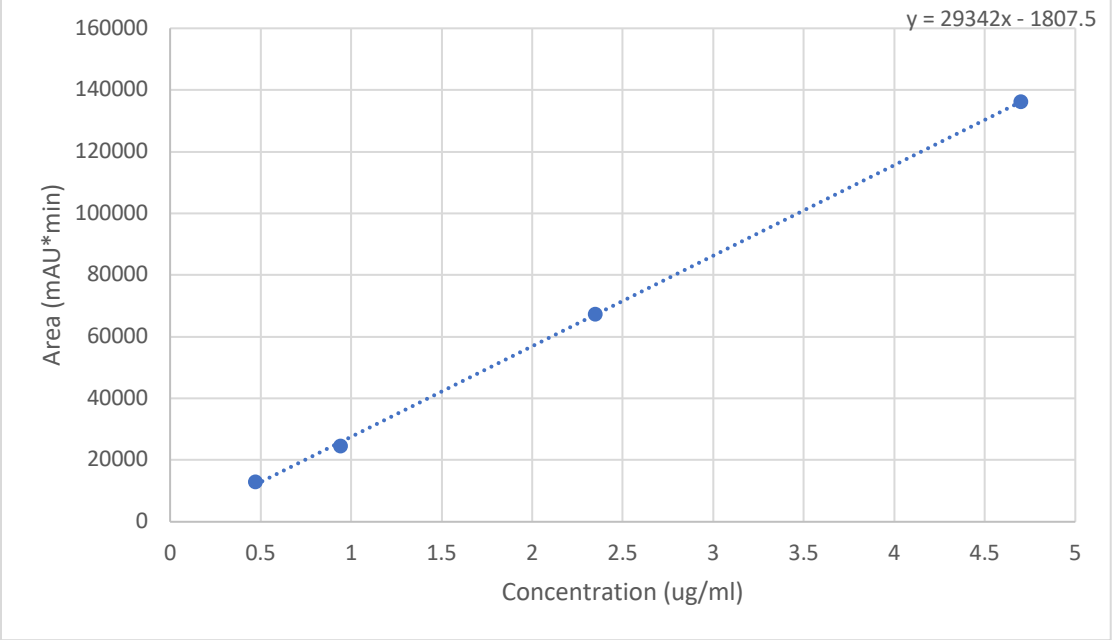

Figure 16. Calibration curve used for following three experiments.

Table 1.7. Quantitative results from the Calibration Curve

Dilutions	*Standard Concentration (µg/mL)*	*Average Area*	*Concentration from slope intercept (µg/mL)*
1:0	4.7	136231	4.70446
1:2	2.35	67374.27	2.35777
1:5	0.94	24651.83	0.90176
1:10	0.47	12902.53	0.50133

The results were used to evaluate the following experiments: *Effect of Dox concentration, Effects of pH and Effects of cobalt concentration.*

Effects of Dox Concentration

The concentration of Dox and its effects on conjugation, was the first of three experiments investigated. The focus of this experiment was to analyze and compare the results on conjugation efficiency when Dox concentration was varied. Four samples were prepared, each with identical amounts of reagents except for Dox. The first sample

prepared contained exactly 47.7 µL of a 5 mg/mL Dox stock solution, and the volume for each subsequent sample was doubled. The relationship between concentration and average peak area was a positive correlation according to HPLC results. The graph confirms that increased amounts of Dox increased the peak intensity, and, furthermore, increased the area beneath the curve. The peak representing 380 µL eluted slightly later than the samples of lesser concentrations (see Figure 17) possibly due to a slight change in HPLC mobile phase composition during the experiment (more solvent had to be mixed and added). At this point, a 500 mL mobile phase container was replaced by a 4 L container to achieve longer run times between mobile phase replenishing. The pooled data (see Table 1.8) shows the quantitative relationship between the amount of Dox and its potential to conjugate. There was very nearly a linear relationship between the amount of Dox added vs. Dox bound (see Figure 18). Furthermore, these results demonstrated our ability to vary the number of Dox molecules bound per protein from 2 to 20, which may have important implications in future development for in vivo models.

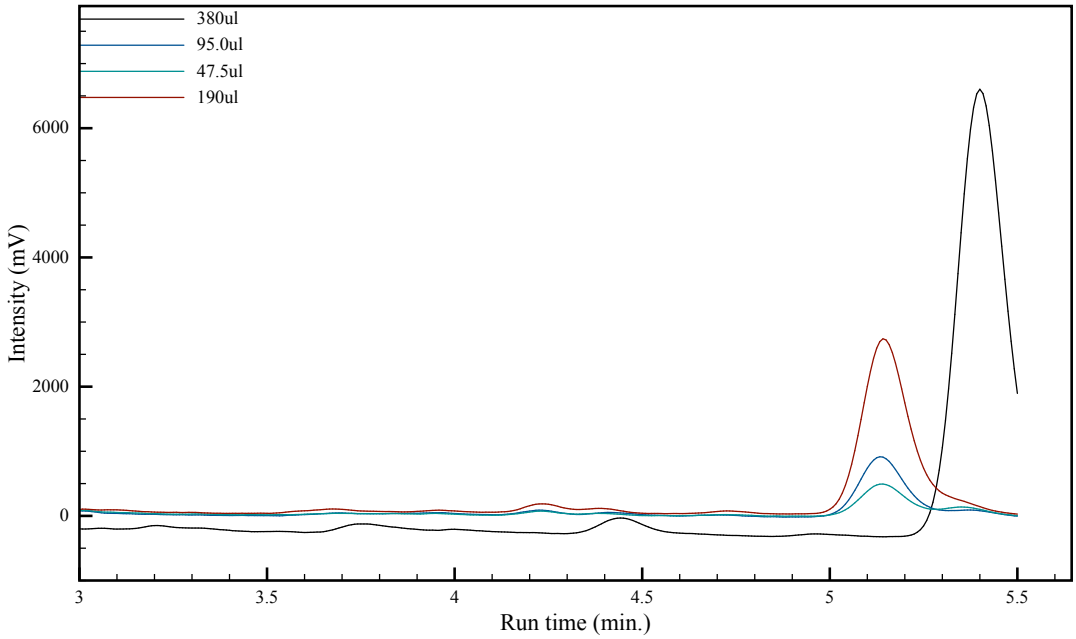

Figure 17. HPLC Chromatograms for samples with varying Dox added during conjugation. The Dox stock solution was 5 mg/mL.

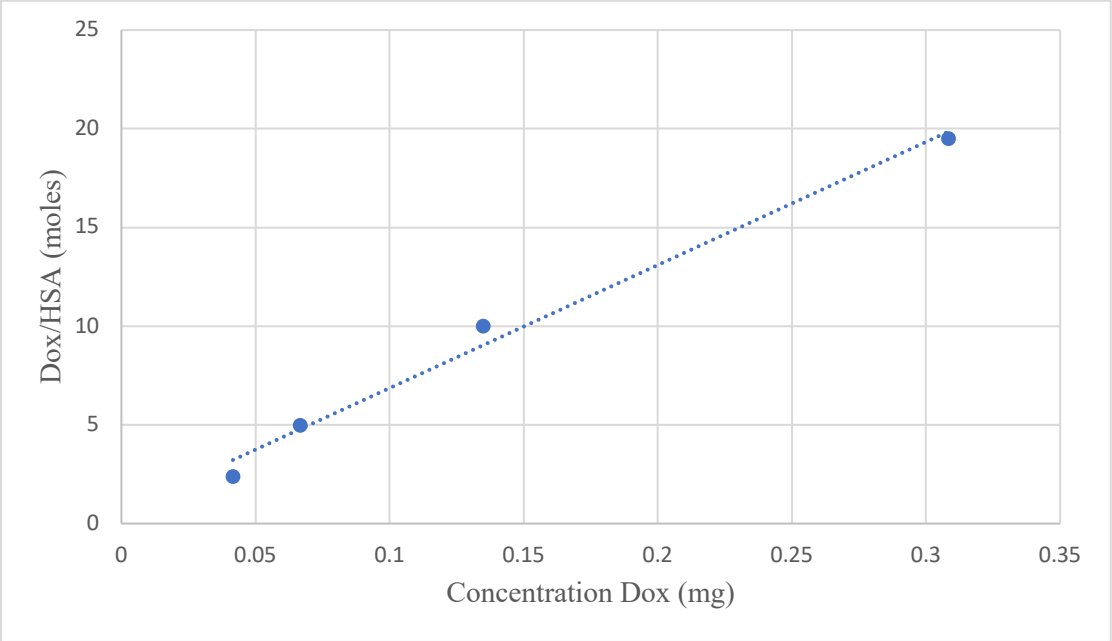

Figure 18. Concentration of Dox vs. HSA

Table 1.8. Results of Various concentrations of Dox after Conjugation

Concentration Dox (µL)	*Average Area*	*Concentration Dox area (µg/mL)*	*Dox released (µg)*	*Dox bound (µg)*	*mol Dox*	*mol Dox/BSA*	*%Dox bound*
47.7	4235.6	0.206	41.60	195.9	$3.60*10^{-7}$	2.40	82.40
95	7880.9	0.330	66.69	408.3	$7.51*10^{-7}$	5.00	85.96
190	21721.9	0.667	134.8	815.2	$1.50*10^{-6}$	10.00	85.81
380	21405.6	1.527	308.4	1592	$2.93*10^{-6}$	19.50	83.77

Effects of pH

The pH experiment was performed to determine if pH variation effected conjugation. The reaction pH was expected to heavily influence conjugation efficiency because the lysine residues on albumin and the amine group on Dox can be protonated in acidic environments and deprotonated in an alkaline environment. Coordination to cobalt requires this lone pair of electrons to be available, so we expected to see higher conjugation efficiency at higher pH where more of the amines would be in their deprotonated state. All samples were prepared with the same 190 µL of Dox (5 mg/mL), 1 mL of BSA (10 mg/mL), and 52 µL of cobalt (0.1 M). For these experiments, the pH was adjusted to either 6, 7, 8, 9 or 10 (see Figure 19). Again, based on previous findings, the pH of samples of BSA and Dox were adjusted separately. The two solutions were then mixed followed by addition of cobalt. The expected trend was observed with the exception of the sample at pH 6. As the pH was raised, conjugation efficiency indeed increased (see Figure 20, Table 1.9). For the sample at pH 6, the lack of release of Dox to the bulk phase was attributed to precipitation that occurred with this sample only. Once precipitation occurs, the Dox remains in the solid state inside the cassette and does not diffuse out into the bulk phase.

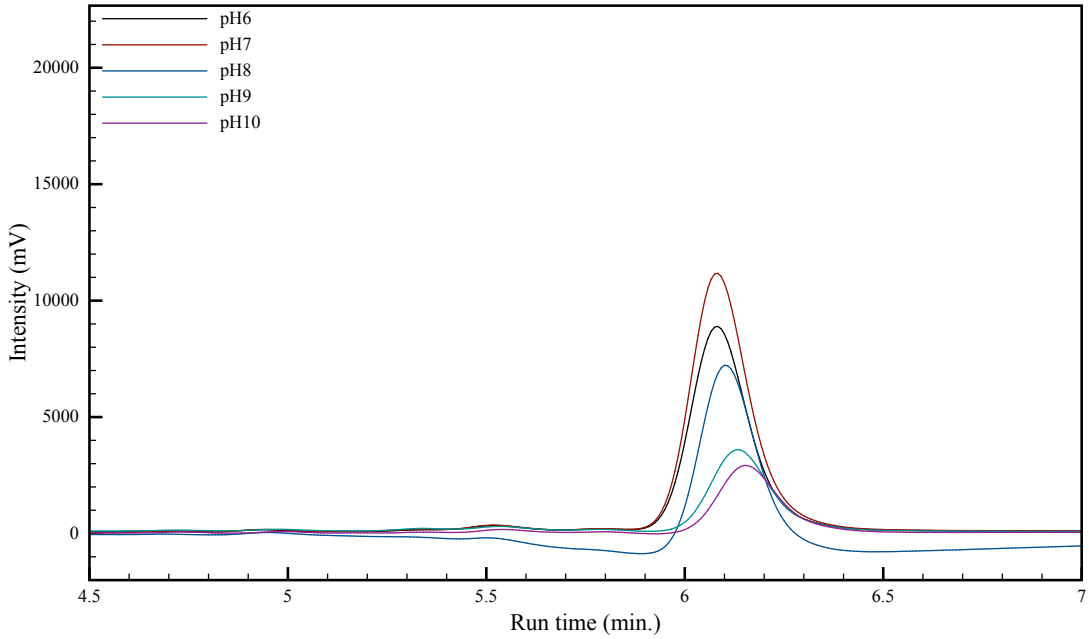

Figure 19. Chromatograms for Dox/BSA conjugation conducted at various pH values.

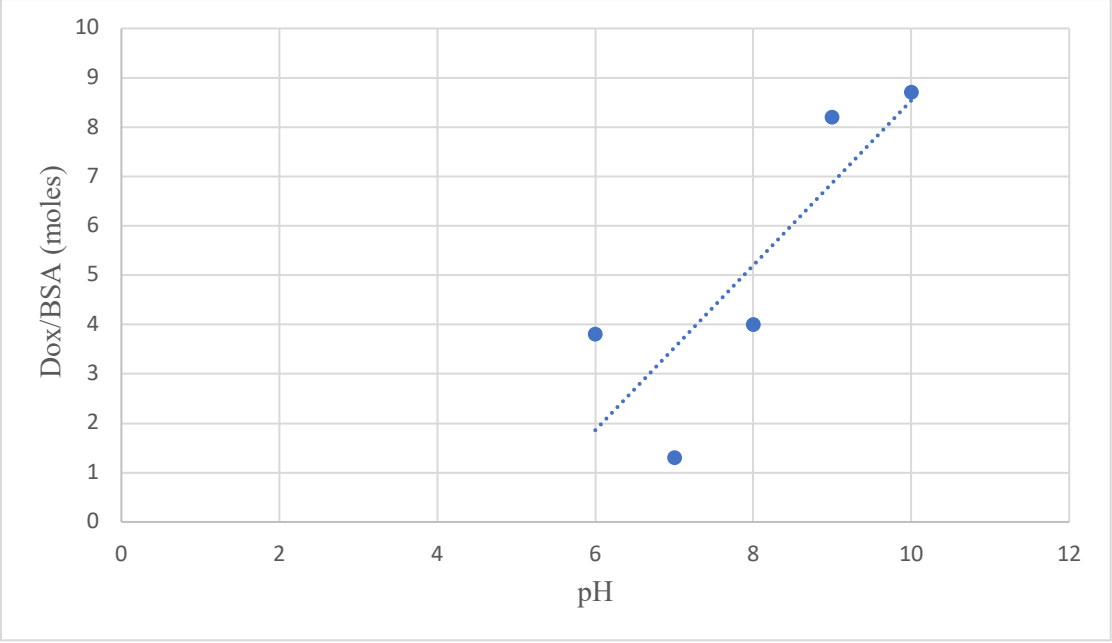

Figure 20. pH vs Dox/BSA

Table 1.9. The pH effects on Dox/BSA conjugation

pH	*Average Area*	*Concentration Dox area (µg/mL)*	*Dox released (µg)*	*Dox bound (µg)*	*mol Dox*	*mol Dox/BSA*	*%Dox bound*
6	91473.5	3.179	642.2	307.8	$5.70*10^{-7}$	3.8	32.40
7	120334.3	4.163	840.9	109.1	$2.00*10^{-7}$	1.3	11.48
8	88616.7	3.082	622.5	327.5	$6.00*10^{-7}$	4.0	34.47
9	39358.6	1.403	283.4	666.6	$1.23*10^{-6}$	8.2	70.16
10	32635.8	1.177	237.1	712.9	$1.31*10^{-6}$	8.7	75.04

Effect of Cobalt Concentration

The varying amounts of cobalt were investigated to observe the effects each addition would have on the polymer-prodrug conjugate. $CoCl_2 \bullet 6H_2O$ was added to each sample in various amounts and incubated for ~72 hours. All of the data in Table 1.10 was computed using the standard equation obtained from Figure 16. $CoCl_2 \bullet 6H_2O$ is a coordinated complex that acts as a linker between our polymer and prodrug. We expected an increase in cobalt concentration (the crosslinker) to the increase Dox binding. The data in Table 1.10 supports this theory. There was a gradual increase in molecules bound to BSA as the amount of cobalt increased (see Figure 21). The sample with 0 µL of cobalt had 6.35 molecules of Dox/BSA, which was again problematic since no crosslinker was present and is an area being further investigated. The four samples that contained cobalt resulted in higher binding activity as expected. We expected to see a stronger trend between the amount of cobalt added and binding efficiency. These experiments were repeated as described below.

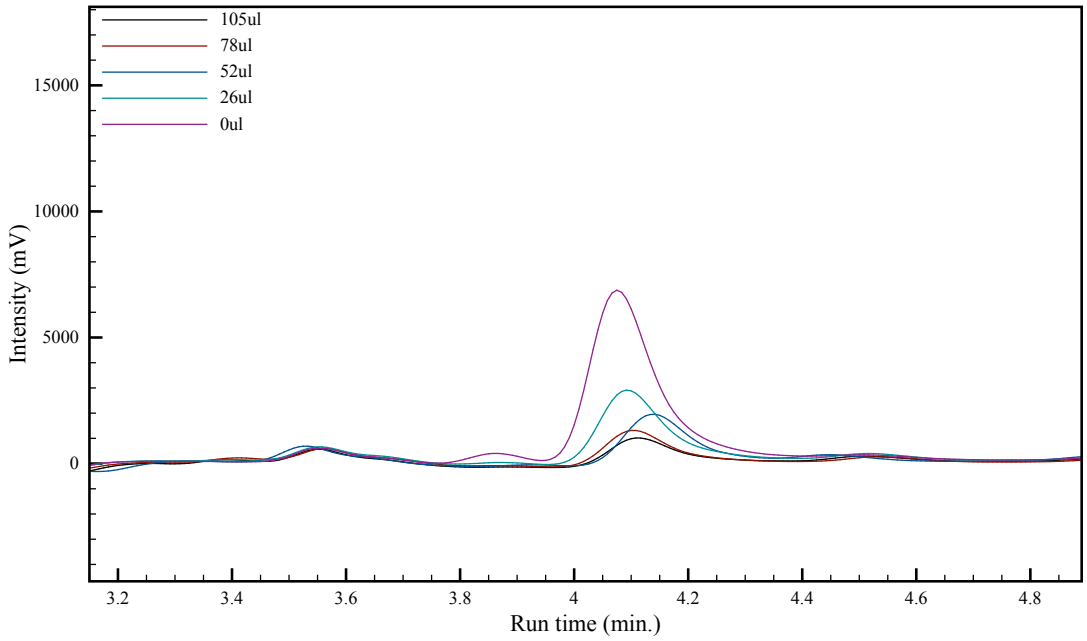

Figure 21. Chromatograms for Dox/BSA conjugation conducted with the addition of varying amounts of cobalt.

Table 1.10. Results of the effect of added cobalt on conjugation efficiency.

Concentration Co (µL)	*Average Area*	*Concentration Dox area (µg/mL)*	*Dox released (µg)*	*Dox bound (µg)*	*mol Dox*	*mol Dox/BSA*	*%Dox bound*
0	60952.7	2.14	432.3	517.7	$9.53*10^{-7}$	6.35	54.41
26	24731.9	0.904	182.6	767.4	$1.41*10^{-6}$	9.4	80.78
52	17091.5	0.644	130.1	819.9	$1.51*10^{-6}$	10.06	86.30
78.5	11555.3	0.455	91.9	858.1	$1.58*10^{-6}$	10.53	90.33
105	10204.6	0.409	82.6	867.4	$1.59*10^{-6}$	10.6	91.31

Effects of Dox Concentration: Utilizing Separate Standards

This experiment was performed to test the reproducibility of adding various concentrations of Dox to HSA. Variables and parameters were standardized in

anticipation of future publications. The data for this experiment was produced using the calibration curve results in Figures 22-23. A new set of standards were prepared and used in this experiment. The equation was utilized as an analyzing tool for the data seen in Table 1.11.

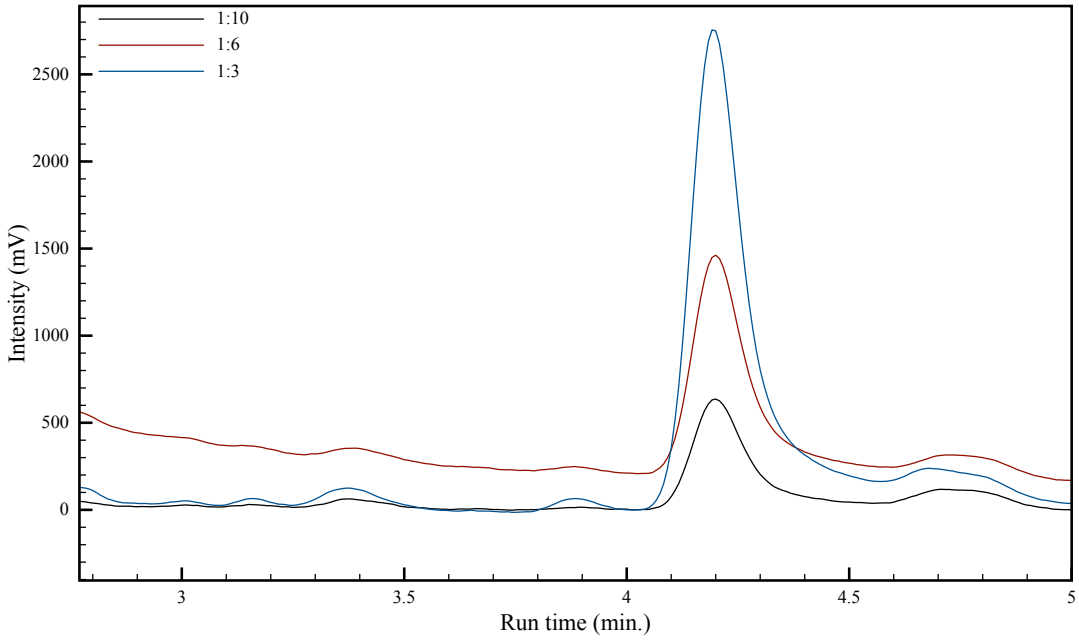

Figure 22. Chromatograms for the standards used to generate a calibration curve for the effects of Dox concentration experiment.

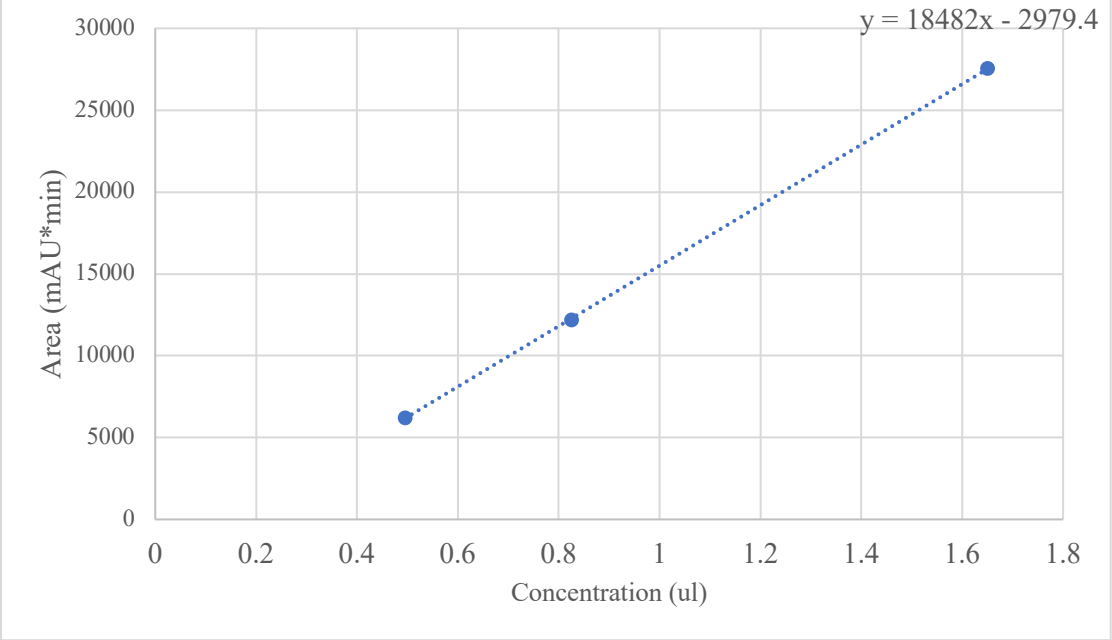

Figure 23. Calibration curve for the effects of Dox concentration.

Table 1.11. Calibration Curve data for the effects of Dox concentration

Dilutions	*Standard Concentration (µg/mL)*	*Average Area*	*Concentration from slope intercept (µg/mL)*
1:3	1.65	27535.4	1.65105
1:6	0.825	12201.26	0.82137
1:10	0.495	6217.2	0.49759

The chromatograms shown in Figure 24 shows that a peak eluted for each sample eluted at ~4.2 min. The concentration of Dox added and the molecules of Dox/HSA remained directly proportional. As seen in Figure 24, a 50% increase in concentration (50 µL to 100 µL) correlated with the 50% increase in molecules of Dox/HSA (2.58 to 5.49) (see Table 1.12). These results support previous observations of an almost linear

relationship between the amount of Dox added and Dox bound under these conditions (see Figure 25).

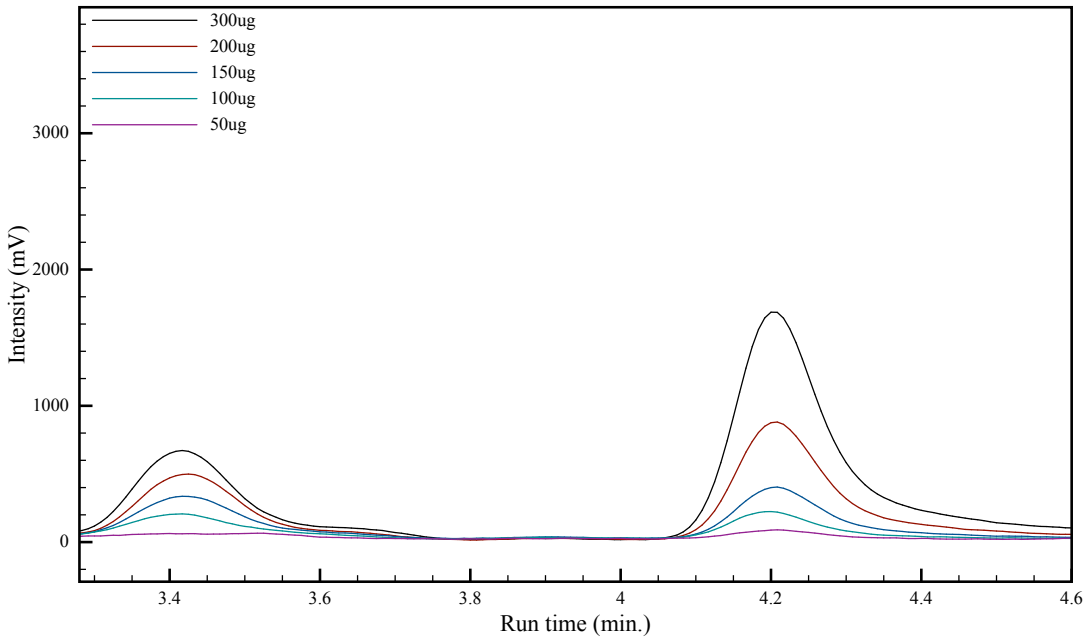

Figure 24. The HPLC results for the effects on Dox concentrations. Peaks at 4.2 min represent Dox samples and peaks at ~3.4 min represent cobalt.

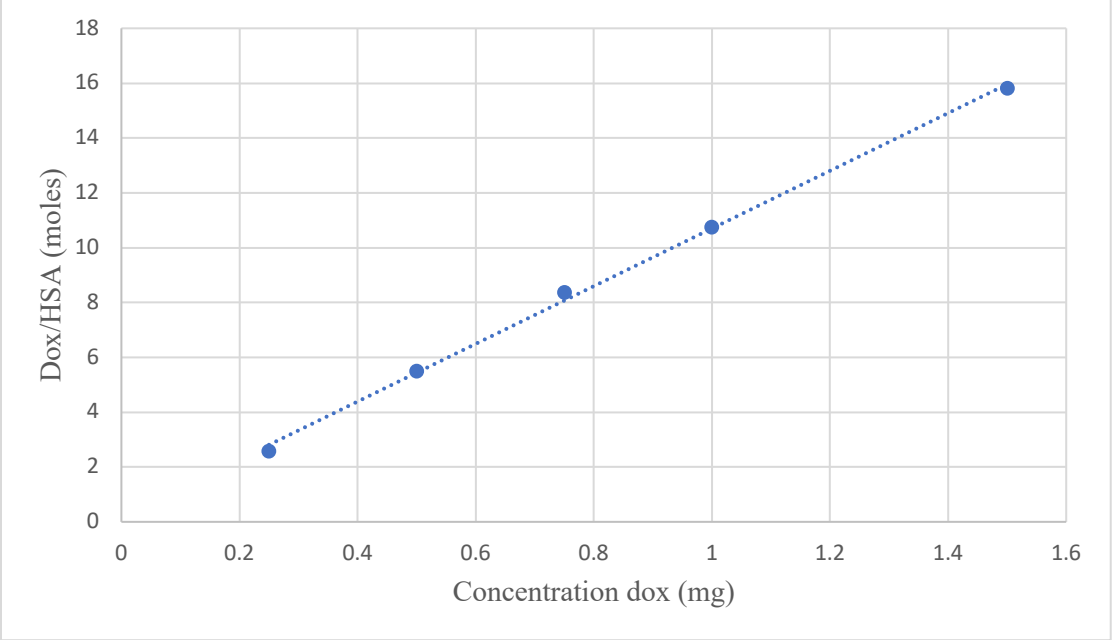

Figure 25. Concentration of Dox vs. Dox/HSA

Table 1.12. Quantitative Results for the Various volumes of Dox

Concentration Dox (µL)	*Average Area*	*Concentration Dox area (µg/mL)*	*Dox released (µg)*	*Dox bound (µg)*	*mol Dox*	*mol Dox/HSA*	*%Dox bound*
50	653.7	0.196	39.71	210.3	$3.80*10^{-7}$	2.58	84.12
100	1745.17	0.256	51.64	448.4	$8.25*10^{-7}$	5.49	89.67
150	3315.7	0.341	68.80	681.2	$1.25*10^{-6}$	8.36	90.83
200	8395.17	0.615	124.3	875.7	$1.61*10^{-6}$	10.74	87.60
300	16311.6	1.044	210.8	1289.2	$2.37*10^{-6}$	15.81	85.59

Effects of Various pH: Utilizing New Standards

The second trial of experiments with varying pH was conducted similarly to the first. The variables that differed were the use of one set of standards and the exclusion of the sample with a pH of 6. Omitting the sample was based on the precipitation of Dox noted above. Experimental calibration data is shown in Figures 26-27 and Table 1.13.

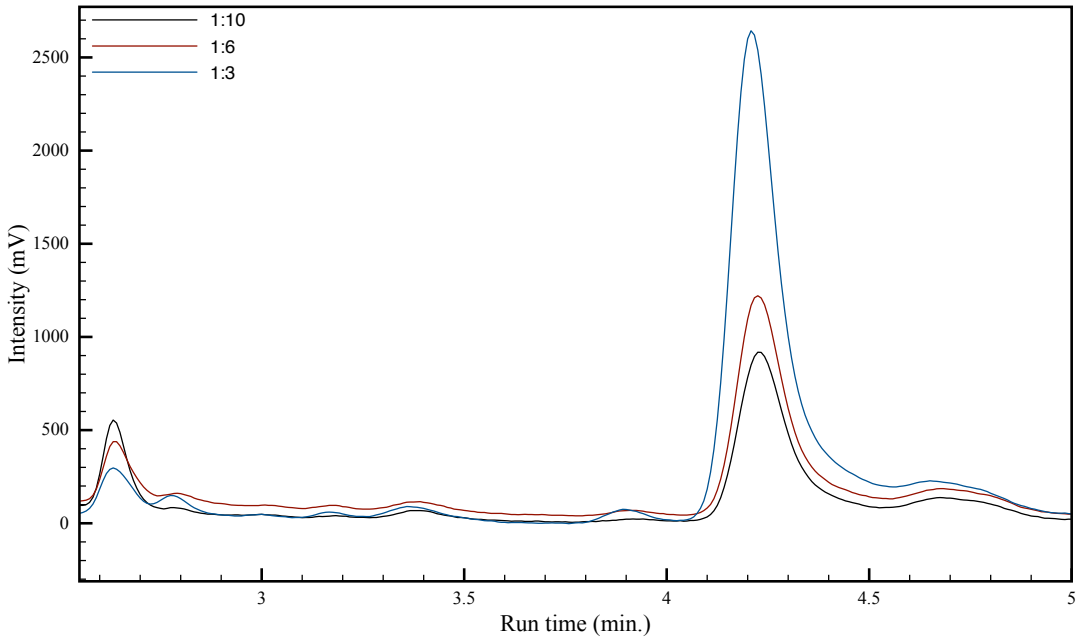

Figure 26. Chromatograms for the standards used to generate a calibration curve for the effects of reaction pH experiment.

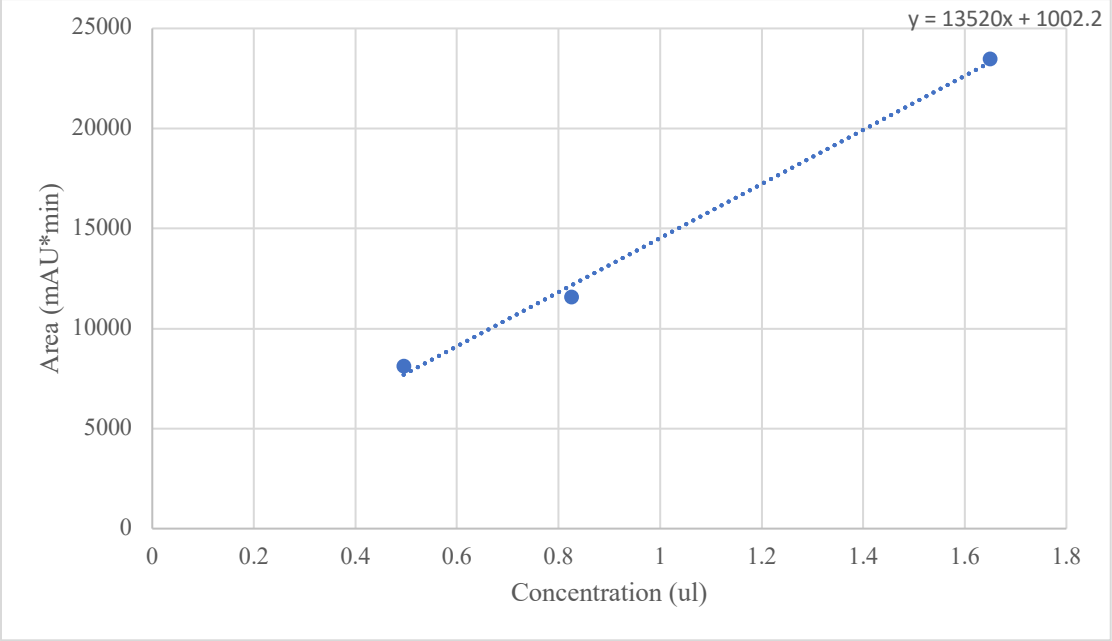

Figure 27. Represents the calibration curve and the standard equation used to calculate the results.

Table 1.13. Calibration Curve for the effects of various pH conditions

Dilutions	*Standard Concentration (µg/mL)*	*Average Area*	*Concentration from slope intercept (µg/mL)*
1:3	1.65	23475.067	1.66071
1:6	0.825	11576.76	0.78147
1:10	0.495	8108.13	0.52558

Conjugation efficiency as a function of pH is shown in Figure 28 and Table 1.14. The samples displayed a peak eluting from the column at ~4.3 min that was a consistently narrow peak. The sample with a pH of 7 had the largest peak and highest values for average area. This correlates with higher amounts of Dox molecules not bound to HSA. The sample run at pH 8 showed a small increase in Dox/HSA binding. The samples run at pH 9 and 10 displayed the most positive results due to the deprotonation of the lysine residues. Again, as expected, increasing pH leads to better conjugation efficiency (see Figure 29).

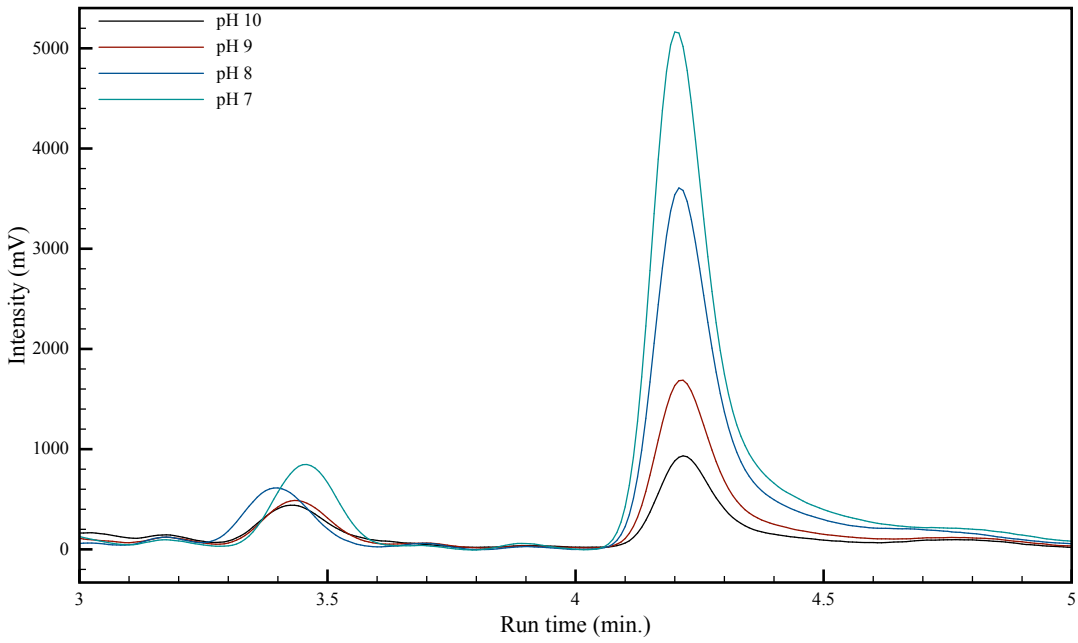

Figure 28. Chromatogram for the 4 samples prepared under varying pH conditions.

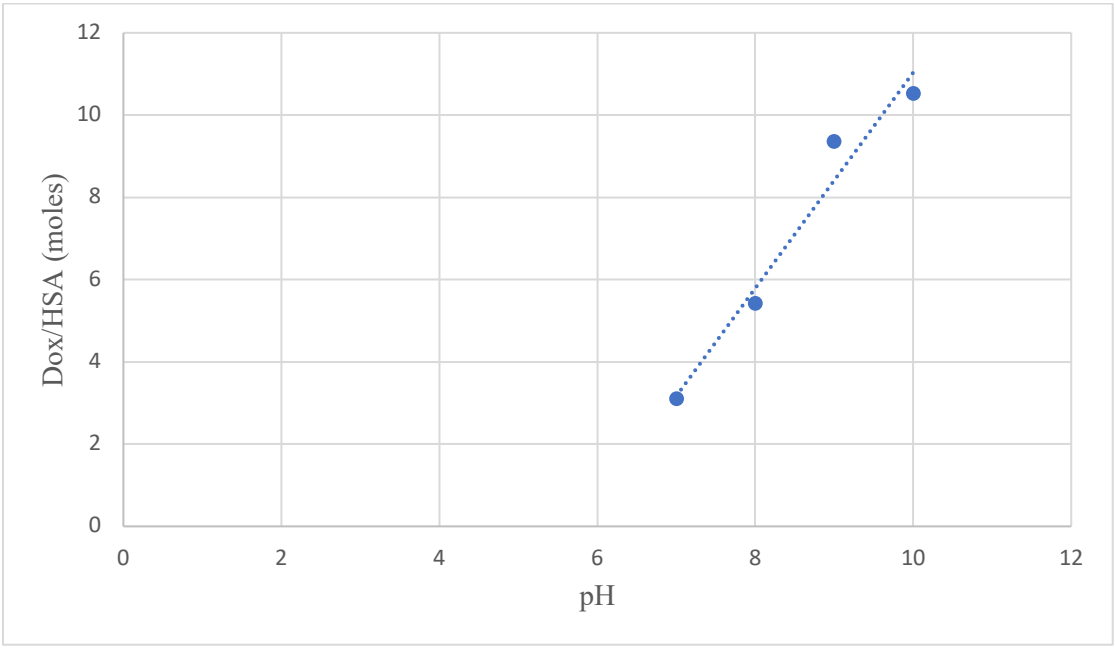

Figure 29. pH vs. Dox/HSA

Table 1.14. Various pH values tested on the Dox/HSA conjugate

pH	*Average Area*	*Concentration Dox area (µg/mL)*	*Dox released (µg)*	*Dox bound (µg)*	*mol Dox*	*mol Dox/HSA*	*%Dox bound*
7	50106.17	3.69	747.13	252.8	$4.65*10^{-7}$	3.10	25.28
8	37473.87	2.76	558.39	441.6	$8.13*10^{-7}$	5.42	44.16
9	15904.53	1.16	236.13	763.8	$1.41*10^{-6}$	9.36	76.38
10	9285.87	0.679	137.24	862.7	$1.58*10^{-6}$	10.53	86.27

Effect of Cobalt Concentration: Utilizing New Standards

The cobalt experiment was conducted to test the reproducibility of the results from above. It was performed to test that an increase in cobalt concentration increased binding. The only parameter that was altered, for this experiment, was added cobalt. The amounts were increased in order to prove a direct relationship between cobalt concentration and conjugation. All new standards were used (see Figures 30-31, Table 1.15) to obtain data seen in Table 1.16.

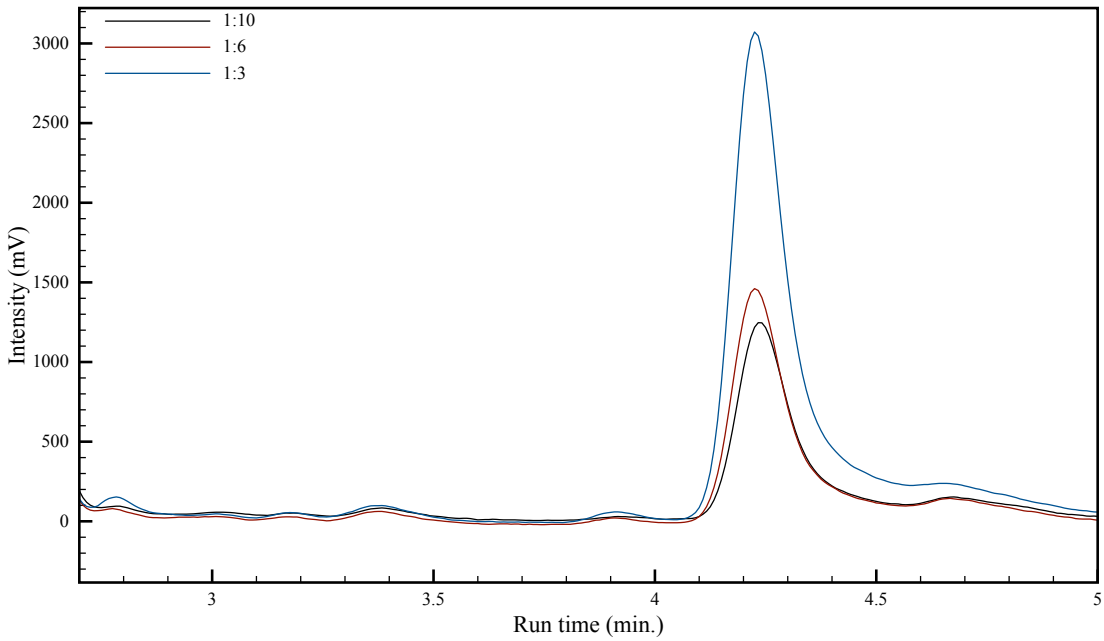

Figure 30. Chromatograms for the standards used to generate a calibration curve for the effects of cobalt concentration on conjugation efficiency experiment.

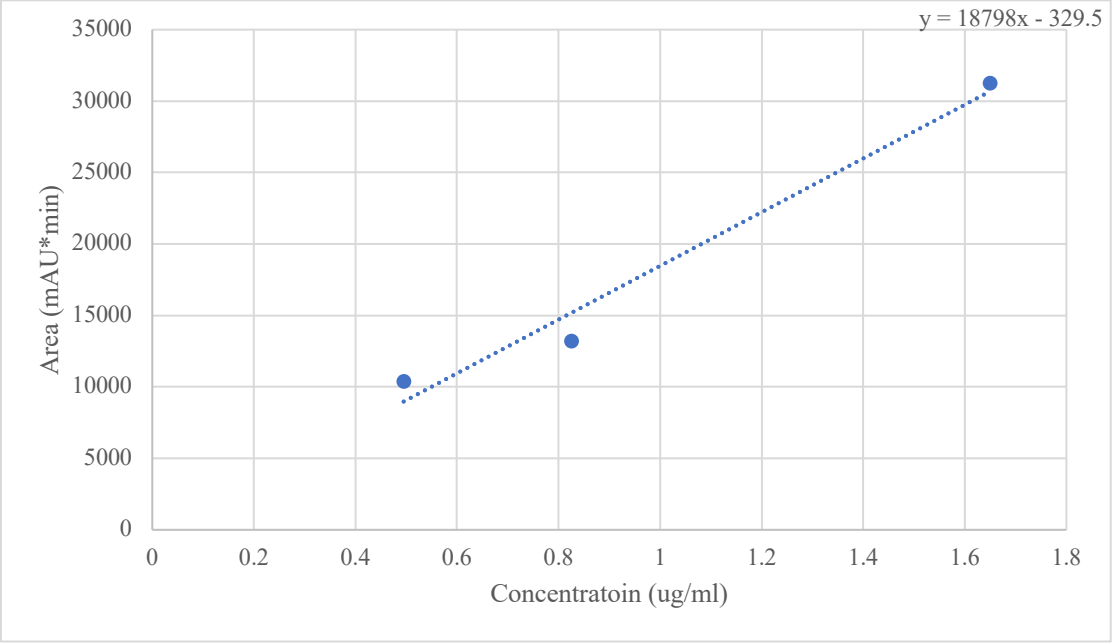

Figure 31. Calibration curve for the effects of cobalt at various concentrations.

Table 1.15. Calibration Curve for the effects of Various amounts of cobalt

Dilutions	*Standard Concentration (µg/mL)*	*Average Area*	*Concentration from slope intercept (µg/mL)*
1:3	1.65	31249.73	1.48233
1:6	0.825	13210.97	0.66658
1:10	0.495	10381.3	0.34826

The sample with 0 µL of Co again exhibited considerable binding (see Figure 32, Table 1.16). Furthermore, there was little correlation between the amount of Dox bound and cobalt added. These results were unexpected and will be the subject of future experiments.

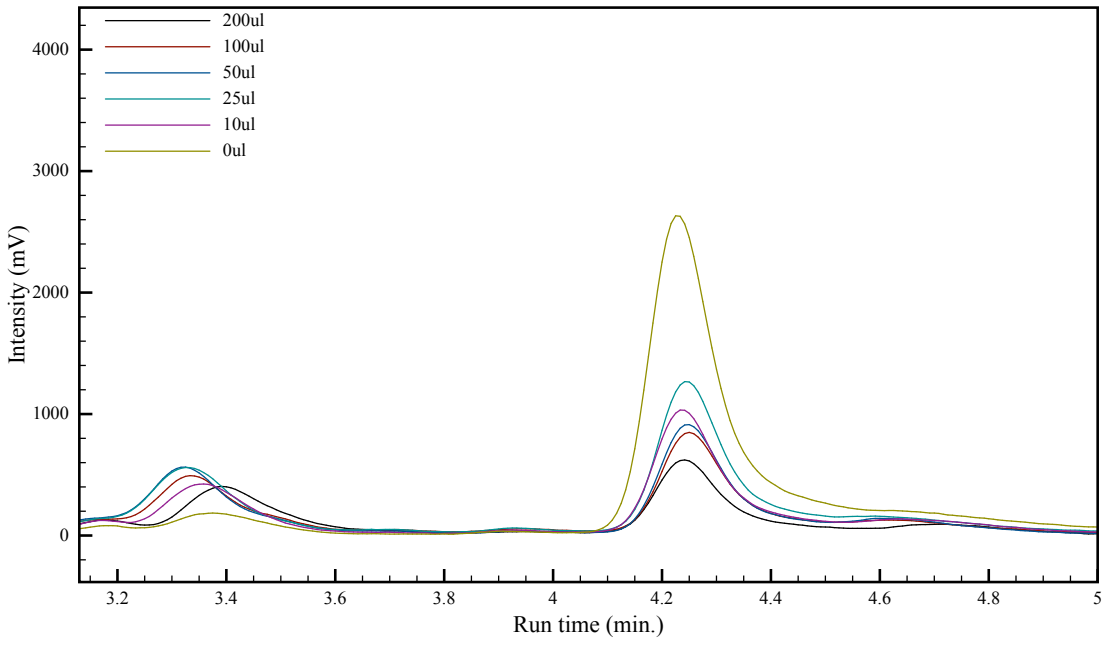

Figure 32. Chromatogram displays results of the effect of cobalt concentration on conjugation.

Table 1.16. Various concentrations of cobalt added to Dox-HSA conjugate.

Concentration Co (µL)	*Average Area*	*Concentration Dox area (µg/mL)*	*Dox released (µg)*	*Dox bound (µg)*	*mol Dox*	*mol Dox/HSA*	*%Dox bound*
0	27482.3	1.444	291.7	708.3	$1.30*10^{-7}$	8.67	70.83
10	9699.0	0.4984	100.7	899.3	$1.65*10^{-6}$	11.00	89.93
25	11003.1	0.5678	114.7	885.3	$1.63*10^{-6}$	10.87	88.53
50	9376.4	0.4813	97.23	902.7	$1.66*10^{-6}$	11.07	90.28
100	7189.2	0.3649	73.71	926.3	$1.70*10^{-6}$	11.33	92.63
200	5555.7	0.2780	56.16	943.8	$1.73*10^{-6}$	11.53	94.38

Dynamic Light Scattering Studies

Effects of Cobalt Concentration: DLS Analysis

Dynamic light scattering was used to confirm that there was no protein aggregation in our samples as a result of the bioconjugation reaction, and that the average size distribution was relatively uniform. This set of experiments used the same samples utilized in HPLC experiments detailed in Figure 32. As can be seen in Table 1.17 no aggregation was apparent with monodispersity being observed for each sample. The average particle size was larger than the overall uniformity, or PDI, of each sample. If the size of the particles is larger than the uniformity of the particles, the sample is considered monodisperse. The best example of this was the sample where 25 µL of Co was added (see Figure 33). The Z-average, or average size of the protein, was 4.54 nm, which was lower than that observed for other samples. Similar to the gaussian distribution, the 10 and 95 percentiles display the protein size at the lowest and highest standard deviations. The lowest deviation range, or the 10 percentile, was 3.58 nm. The highest deviation range, or the 95 percentile, was 7.42 nm. The percentiles help to support monodispersity

because it confirmed the range of the size distribution. Because this sample had a low Z-average and very little deviation, the calculated PDI was also low. Furthermore, when comparing the average particle size (4.54 nm) to the PDI (0.959), this sample displayed good monodispersity.

Table 1.17. The DLS data for varying amount of Cobalt added

Concentration Co (µL)	*Standard Deviation*	*Polydispersity Index*	*Z-Average*	*10% (nm)*	*95 % (nm)*
10	1.100	0.944	5.13	4.18	8.03
25	1.090	0.959	4.54	3.58	7.42
50	1.240	0.899	5.16	3.92	8.32
100	1.320	1.145	5.61	4.52	9.41
200	2.630	0.594	4.98	2.10	10.45

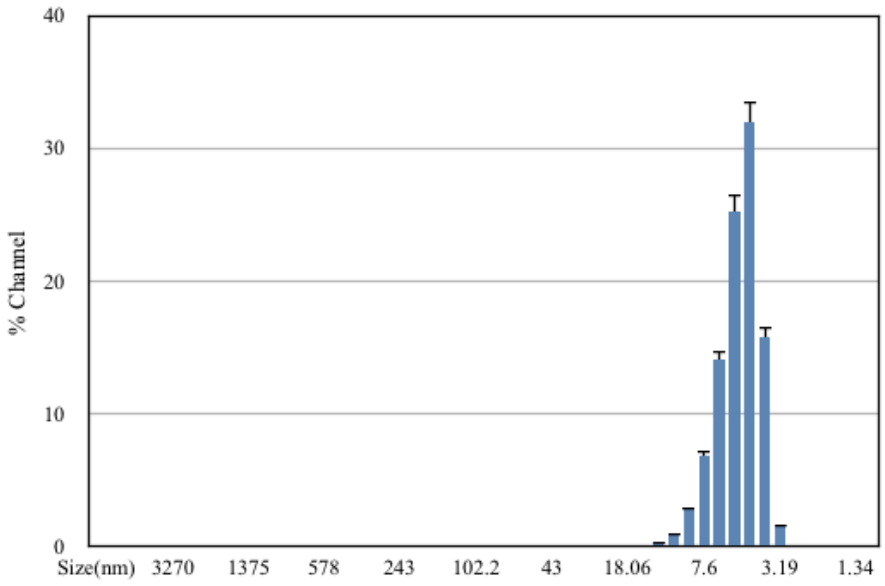

Figure 33. DLS results for varying cobalt concentration (25 µL added).

The sample prepared with 200 µL added of Co added exhibited the least monodispersity (see Figure 34). Although the PDI (0.594) and the Z-average (4.98) show

good monodispersity, the standard deviation (2.63) was the highest of all 5 samples observed. Because the 10th and 95th percentile deviations were so high, it was apparent that the standard deviation would also be high. The 10th percentile resulted in 2.10 nm and the 95th percentile was 10.45 nm. Since the PDI was lower than the Z-average, overall, the data was considered acceptable.

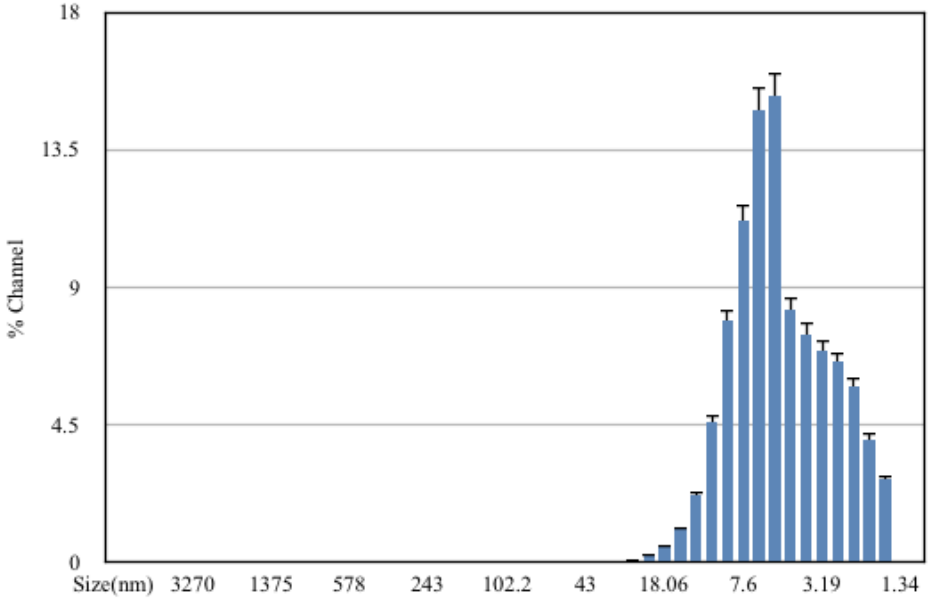

Figure 34. DLS results for varying cobalt concentration (200 µL added).

Effects of Dox Concentration

The sample that displayed the most monodispersity was after addition of 150 µL of Dox (see Figure 35). The PDI was 0.491 and the Z-average was 5.19 (see Table 1.18). The data illustrates the uniformity in both size and shape. This was a result of the Z-average being larger than the PDI value. The sample containing 50 µL of added Dox showed the lowest monodispersity with a PDI of 0.406 and a Z-average of 7.50 nm (see Figure 36). The PDI was lower than the Z-average, which shows monodispersity, but

values also exhibited very high deviations. The 10th and 95th percentiles are high for this sample, 5.30 nm and 15.52 nm, respectively. As a result, the standard deviation was higher, meaning the uniformity was lower for this sample.

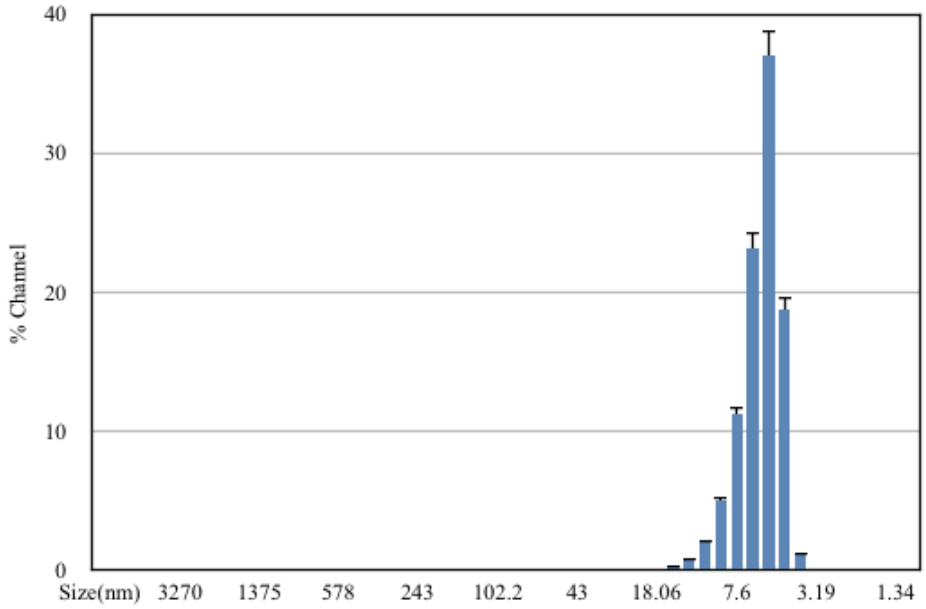

Figure 35. DLS results for varying Dox concentration (150 µL added).

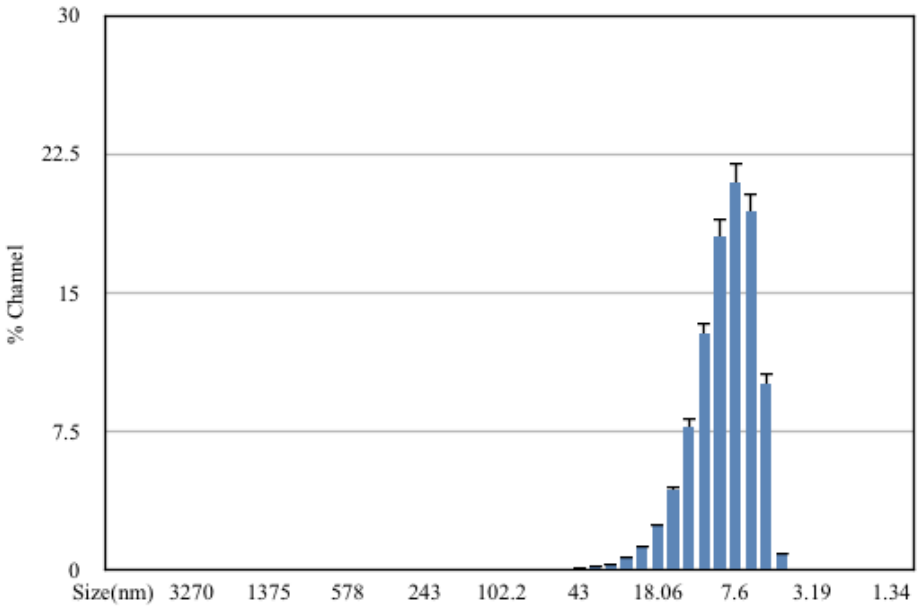

Figure 36. DLS results for varying Dox concentration (50 µL added).

Table 1.18. The DLS data for the varying amount of Dox added

Concentration Dox (ul)	*Standard Deviation*	*Polydispersity Index*	*Z-Average*	*10% (nm)*	*95 % (nm)*
50	2.710	0.406	7.50	5.30	15.52
100	1.300	0.521	5.37	4.20	9.14
150	1.140	0.491	5.19	4.21	8.43
200	1.200	0.581	5.04	4.04	8.29
300	1.250	0.617	5.56	4.34	8.93

Effects of pH on Protein Stability

Protein stability was analyzed for reactions run at four pH values. Each sample's PDI and Z-average data were consistent with optimal protein dispersity (see Figure 37, Table 1.19). The standard deviation was low for each sample and represented uniformity in protein size and shape. The sample run at pH of 8 had the highest standard deviation at

2.09. The 10th and 95th percentiles were also larger in comparison to the other samples observed, ranging from 2.81 nm and 9.05 nm, respectively. Although this is still considered monodispersed, the sample is considered the least uniform. The results lead to the conclusion that changes in reaction pH did not induce protein aggregation and the protein remained stable under all conditions.

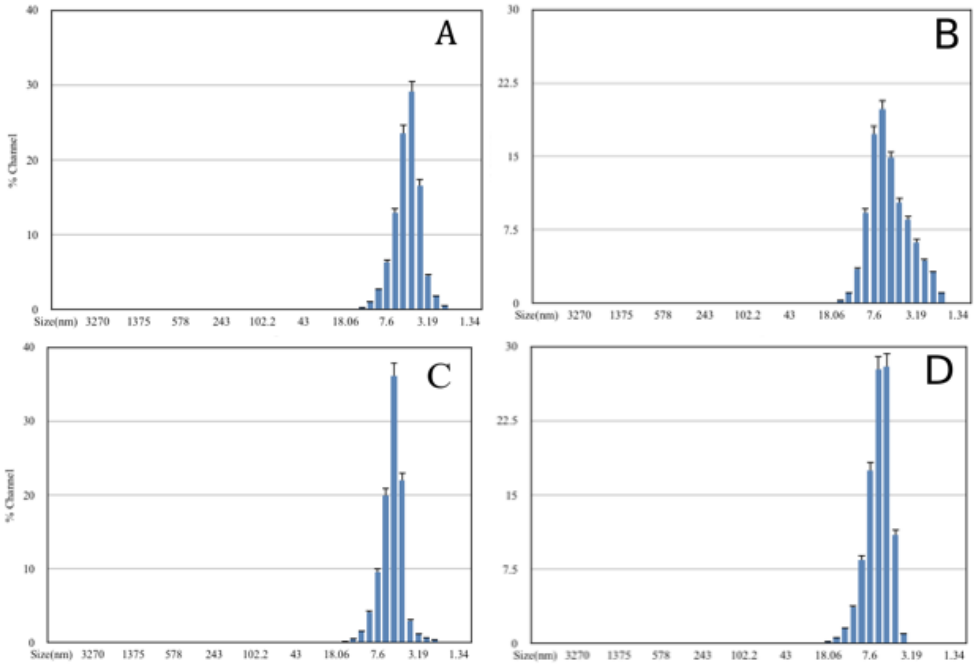

Figure 37. effects of reaction pH on protein stability via dynamic light scattering a. pH 7 b. pH 8 c. pH 9 d. pH 10

Table 1.19. Measured DLS Parameters for effect of reaction pH on protein stability.

pH	*Standard Deviation*	*Polydispersity Index*	*Z-Average*	*10% (nm)*	*95 % (nm)*
7	1.150	0.250	4.45	3.34	7.43
8	2.090	0.537	5.45	2.81	9.05
9	1.110	0.385	5.02	4.00	8.03
10	1.420	0.554	5.70	4.43	9.48

CHAPTER IV

CLOSING STATEMENTS

My experience doing research at Texas Woman's University has taught me to think openly when it comes to all sciences. It is true that chemistry, biology and physics are all separate fields, but some theories overlap. I have learned that targeted drug delivery is best understood, broadly, as a biological tool that can be used to treat cancer. I now understand the structure of a protein-drug conjugate is based on its chemical bonds. I can also appreciate the amount of physics that is used to understand Dynamic Light Scattering. Understanding that science is not limited to a single field or theory, is the most powerful tool a scientist can possess.

I once believed that I would never be a part of something bigger than I am. Although our research is conducted in a small lab on a small campus, what we do could one day be of great significance. In the book *The Emperor of all Maladies*, Mukherjee quotes Saint Aquinas, "The more perfect a power is, the more difficult it is to quell."[22] I do not believe cancer is a perfect power, but I do believe we will find its imperfections and one day conquer it.

REFERENCES

[1] Zhou, Q.; Zhang, L.; Wu, H. Nanomaterials for Cancer Therapies. *Nanotechnology Reviews*. **2017**; *6* (5), 473-496.

[2] World Health Organization. *Noncommunicable diseases and their risk factors*. [Online] **2018**. http://origin.who.int/ncds/en/ (accessed 2019-12-2).

[3] Odularu, A. T. Metal Nanoparticles: Thermal Decomposition, Biomedicinal Applications to Cancer Treatment, and Future Perspectives. *Bioinorg Chem Appl*. **2018**, *2018* (9354708), 1-6.

[4] Barry, J. N.; Vertegel, A. A. Nanomaterial for Protein-Mediated Therapy and Delivery. *Nano Life.* **2013**; *3*(4).

[5] Petros, R. A.; Desimone, J. M. Strategies in the Design of Nanoparticles for Therapeutic Applications. *Nat. Rev. Drug Discov.* **2010**; *9*, 615-627.

[6] Nguyen, D. T.; Cavazos, R. J.; Harris, A. N.; Petros, R. A. Werner Complexes Viewed Anew: Utilizing Cobalt Coordination Chemistry for 'Traceless' Stimuli-Responsive Bioconjugation Involving Therapeutic Nanoparticles, Protein PEGylation, and Drug-(Bio)Polymer Conjugates. *Comments Inorg. Chem.* **2014**; *34* (3-4), 59-77.

[7] Doxorubicin. *The Myeloma Beacon*. [Online] Beacon Foundation for Health. Aug 8, **2008.** http://myelomabeacon.org/resources/Dox/ (accessed 2019-12-2).

[8] US National Library of Medicine. *National Center for Biotechnology Information*. Pub Chem. Home Page. Doxorubicin. [Online] https://pubchem.ncbi.nlm.nih.gov/compound/Doxorubicin (accessed 2019-12-2).

[9] Kratz, F. Albumin as a Drug Carrier: Design of Prodrugs, Drug Conjugates and Nanoparticles. *J. Control. Release* **2008**; *190*, 331-336.

[10] Hawkins, M. J.; Soon-Shiong, P.; Desai, N. Protein Nanoparticles as Drug Carriers in Clinical Medicine. *Adv. Drug Deliv. Rev*. **2008**; *60* (8), 876-885.

[11] Hoang, H.; Manyanga, Fidelis Morakinyo, M. K.; Vincent, P.; Ferdous, S.; Fish, D. J.; Brewood, G.; Benight, A. S. Effects of Selective Biotinylation on the Thermodynamic Stability of Human Serum Albumin. *J. Biophys. Chem.* **2016**; *7*, 9-29.

[12] Mo, R.; Jiang, T.; Disanto, R.; Tai, W.; Gu, Z. ATP-Triggered Anticancer Drug Delivery. *Nat. Commun.* **2014**; *5* (3364), 1-10.

[13] Goodman, A. M.; Neumann, O.; Nørregaard, K.; Henderson, L.; Choi, M. R.; Clare, S. E.; Halas, N. J. Near-Infrared Remotely Triggered Drug-Release Strategies for Cancer Treatment. *Proc. Natl. Acad. Sci. U. S. A.* **2017**; *114* (47), 12419-12424.

[14] Manzoor, A. A.; Lindner, L. H.; Landon, C. D.; Park, J. Y.; Simnick, A. J.; Dreher, M. R.; Das, S.; Hanna, G.; Park, W.; Chilkoti, A.; et al. Overcoming Limitations in Nanoparticle Drug Delivery: Triggered, Intravascular Release to Improve Drug Penetration into Tumors. *Cancer Res.* [Online] **2012**; *27*, 5566-5575. DOI: 10.1158/0008-5472 (accessed 2019-12-2).

[15] Gorovits, B.; Krinos-Fiorotti, C. Proposed Mechanism of Off-Target Toxicity for Antibody-Drug Conjugates Driven by Mannose Receptor Uptake. *Cancer Immunol, Immun*. [Online] **2013**; *62*, 217-223. DOI: 10.1007/s00262 (accessed 2020-03-26).

[16] Motlagh, N. S. H.; Parvin, P.; Ghasemi, F.; Atyabi, F. Fluorescence Properties of Several Chemotherapy Drugs: Doxorubicin, Paclitaxel and Bleomycin. *Biomed. Opt. Express* [Online] **2016**.; *7* (6), 2400-2406. DOI: 10.1364/boe.7.002400 (accessed 2020-03-24).

[17] LS Instruments AG. Home Page. [Online] https://lsinstruments.ch/en/technology/dynamic-light-scattering-dls (accessed 2019-12-2).

[18] Siew, A.; Brown, M. Analyzing Protein Aggregation in Biopharmaceuticals. *Pharm. Technol.* [Online] Jan 01, **2015**, *28* (1). http://www.biopharminternational.com/analyzing-protein-aggregation-biopharmaceuticals-0. (accessed 2020-03-26).

[19] Loo, Joseph A.; Rathore, Anurag S.; Krull, I. S. The Current and Future State of Top-down Protein Sequencing by ESI-Tandem Mass Spectrometry. *LCGC North Am.* [Online] **2016**; *34* (6), 493-499. http://www.chromatographyonline.com/current-and-future-state-top-down-protein-sequencing-esi-tandem-mass-spectrometry. (accessed 2019-12-2).

[20] Berne, Bruce J.; Pecora, Robert. Introduction: Historical Sketch. In *Dynamic Light Scattering with Applications to Chemistry, Biology, and Physics;* Dover Publications, Inc, **1977**.

[21] Microtrac: 'Nanotrac Wave II' Family of Particle Size & ZetaPotential Analyzers: Mode; MN42x Operation and Maintenance Manual. *Total Solutions in Particle Characterizations*. **2015**.

[22] Mukherjee, S. *The Emperor of All Maladies: A Biography of Cancer*. J. Postgrad. Med. Educ. Res. **2012**.